Buckling Analysis of Single-walled Carbon Nanotubes (SWCNTs) using Finite Element Method

by

Nor Azlinda Azmi

Dissertation submitted in partial fulfillment of

the requirement for the

Bachelor of Engineering (Hons)

(Mechanical Engineering)

MAY 2012

Universiti Teknologi PETRONAS

Bandar Seri Iskandar

31750 Tronoh, Perak Darul Ridzuan.

CERTIFICATION OF APPROVAL

Buckling Analysis of Single-walled Carbon Nanotubes (SWCNTs) using Finite Element Method

by

Nor Azlinda Azmi

A Project Dissertation submitted to the

Mechanical Engineering Programme

Universiti Teknologi PETRONAS

in partial fulfillment of the requirement for the

BACHELOR OF ENGINEERING (Hons)

(MECHANICAL ENGINEERING)

Approved by,

_____

(MOKHTAR B. AWANG)

UNIVERSITI TEKNOLOGI PETRONAS

TRONOH PERAK

MAY 2012

CERTIFICATION OF ORIGINALITY

This is to certify that I am responsible for the work submitted in this project that the original work is my own except as specified in the references and acknowledgement, and that their original work contained herein have not been undertaken or done by unspecified sources or persons.

_____

(NOR AZLINDA AZMI)

ABSTRACT

A finite element simulation technique is proposed and developed to investigate the buckling behavior of SWCNTs. SWCNTs are particularly complicated for any mechanical test due to its miniature molecular dimensions. Due to the difficulties of experiments at the nanoscale level, numerical works are conducted to determine the mechanical properties of carbon nanotubes. Numerical works can be divided into two types which are continuum mechanics and molecular dynamics. CNTs are not nearly as strong under compression because of their hollow structures and high aspect ratio. Hence, it is important to find and investigate the buckling behavior of the carbon nanotubes. The simulation is defined based on the concept of equivalence of molecular dynamics and continuum mechanics approach. The buckling behavior of SWCNTs is predicted based on certain application of load consists of the axial loading. A set consisting of four (4) different lengths of armchair SWCNTs is investigated to observe the variation in the buckling behavior. The carbon nanotubes are simulated as a frame-like structure and the model are built using the finite element commercial code ANSYS. The type of element used is non-linear 188 beam element. The result shows various significant variations in buckling behavior for every tube lengths.

ACKNOWLEDGEMENT

This dissertation would not have been possible done without the guidance and helps of several individuals who in directly or indirectly contributed and lend their valuable assistance in the preparation and completion of this final year project.

First and foremost, I would like to express my utmost gratitude to Dr. Mokhtar B Awang, my supervisor for this project. Without his guidance I will never be able to complete the project up to this level. He has been my inspiration as to accept and face all the findings, and new learning also the obstacles in the completion of this research project.

I would also like to thank Mr. Ehsan Mohammadpour, who has been the direct tutor in utilizing ANSYS as a finite element modeler. With his guidance, I can model a desired carbon nanotube and learn the basic learning of using ANSYS software. With his aid also, I managed to tackle the model until the expected results are obtained.

Last but not the least, my family and the one above all of us, God, for answering my prayers for giving me the strength to continue and do not give up in completing this project. Alhamdulillah.

TABLE OF CONTENTS

LIST OF FIGURES AND TABLES

CHAPTER 1

INTRODUCTION

1.1 History of Carbon Nanotubes

The findings of Carbon Nanotubes (CNTs) started in the early 1970s. A scientist who earned his Ph.D in France, Marinobu Endo found a set of carbon filaments. These carbon filaments were firstly entrusted as the CNTs. However, the carbon filaments were failed to meet certain measurements requirements. In 1991, the real first CNTs were discovered by a Japanese scientist, Sumio Iijima. Figure 1 shows the physical appearance of carbon nanotubes.

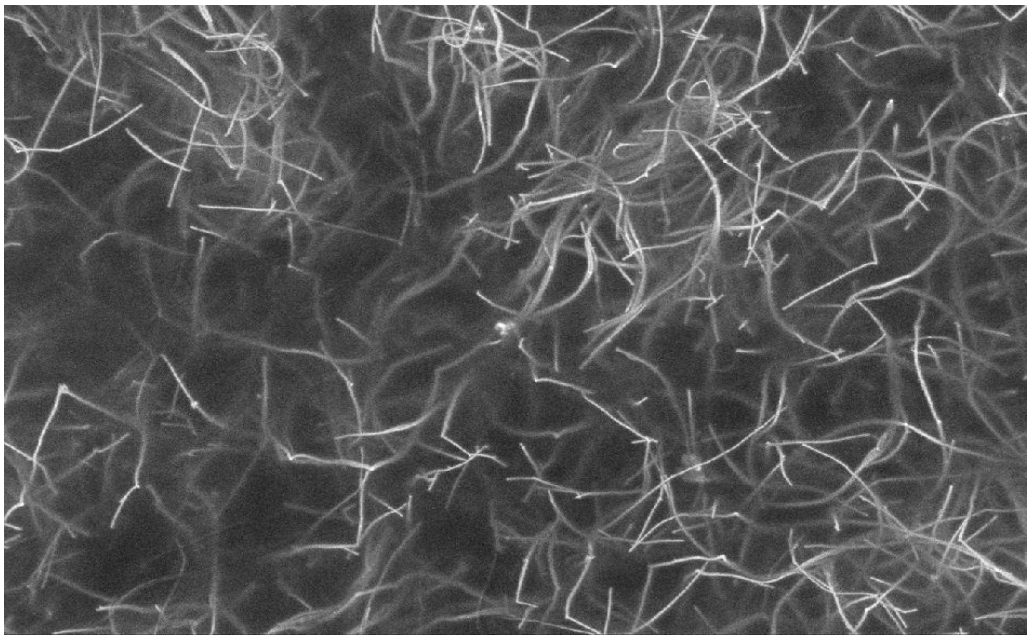

Figure 1: Carbon nanotubes in physical appearance

Their name was originally come from their structure and size. At that time, CNTs were called Multi-walled Carbon Nanotubes (MWCNTs) as shown in Figure 2(b). Two years later, in 1993, Iijima and Donald Bethune discovered a so called Single-walled Carbon Nanotubes (SWCNTs) as shown in Figure 2 (a).

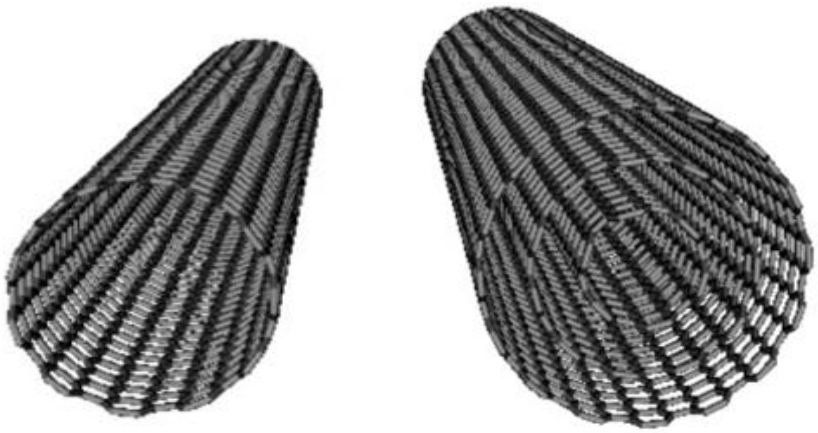

a) **b)**

Figure 2: a) SWCNT and b) MWCNT

1.2 Geometry of Carbon Nanotubes

MWCNT comprises of multiple wall of SWNCT and in the ideal case, a SWCNT can be viewed as a graphene sheet that has been rolled into a tube while a MWCNT is composed of concentric graphitic cylinders with closed caps at both ends and the graphitic layer spacing is about 0.34 nm [1]. Concisely, a SWCNT consists only with one layer of graphene sheet, while MWCNT consists of two or more graphene sheet. Subsequently, a SWCNTs without end-caps, is viewed as tubes with hexagonal carbon rings. One hexagonal ring comprises of six carbon atoms with five covalent bonds. The covalent bonds represent a very strong chemical bond and are the main role in the tube's mechanical properties. The name was originally come from the size of the graphene wall which is equal to one carbon atom thickness in nanometer. Based on figure 3 and 4, there are three types of SWCNTs based on their structural parameters; the armchair, zig-zag and chiral nanotubes. Armchair nanotubes are defined by (n,n), zig-zag is by (n,0) while the chiral arrangement is by (n,m).

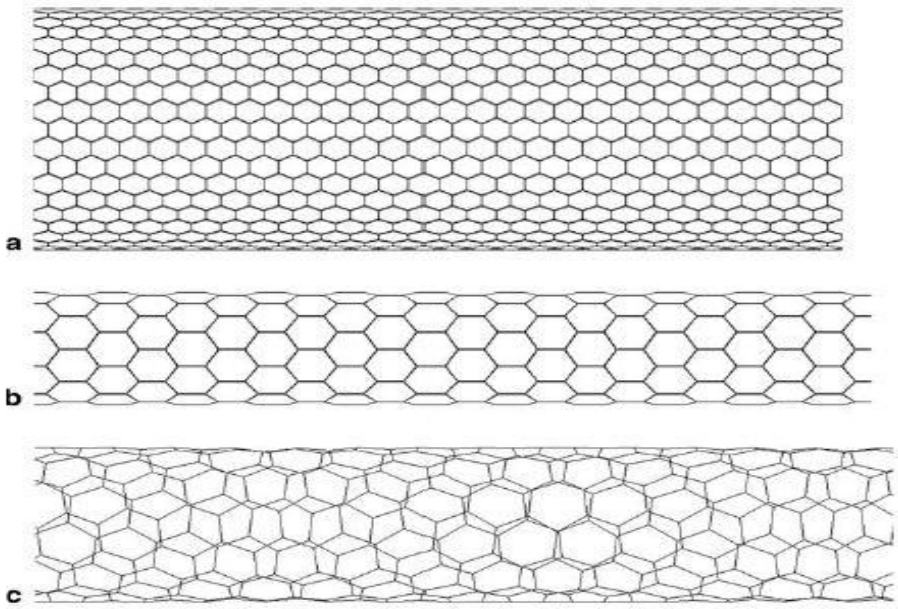

Figure 3: Carbon nanotube: a) armchair (b) zig-zag (c) chiral [2]

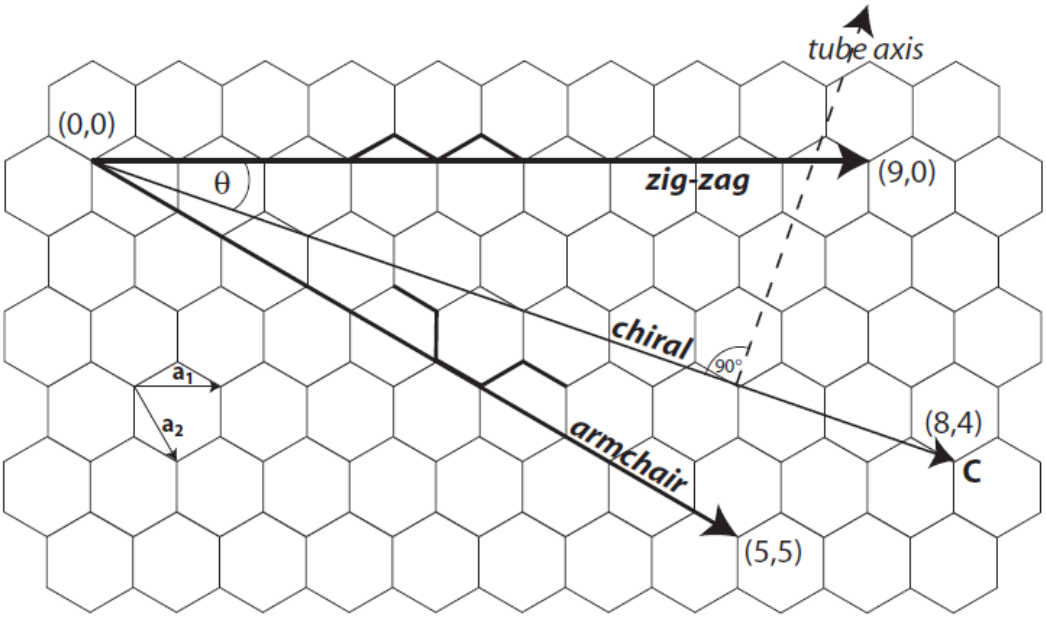

Figure 4: Geometry of a CNT of a two-dimensional graphene sheet

1.3 Potential Applications of Carbon Nanotubes

The discovery of CNTs has developed several ideas in engineering materials science field. These cylindrical carbon molecules have extraordinary properties, which are seen to have benefits in nanotechnology, electronics, optics and other areas of engineering materials.

Above all, due to their potentially thermal conductivity, mechanical and electrical properties, carbon nanotubes discover function as reinforce element to various structural materials. For example, most polymers are made of carbon and have low density. However, they are frequently consisting of weak bonds between their chains and as a result, they are not strong. This can be reinforced by forming polymers composites with other stiff materials such as carbon nanotubes. It has been demonstrated that with only 1% (by weight matrix) of carbon nanotubes added in matrix material, the stiffness of the resulting composite film can increase by 36-42%, while the tensile strength by 25% [2].

Other than that, carbon nanotubes have high potential as material for electrical equipment. Among the findings are such as the transistors, wires, cables, solar cells elements and capacitors. In medical science, CNTs are seen to have potential as the material in structuring the human bones. Besides that, a research is conducted to investigate the potential of using CNTs as cancer healer medium. This is by using the CNTs as a drug delivery. Current cancer therapy mainly comprises surgery, radiation therapy, and chemotherapy. These procedures of treatment are usually painful and destroy normal cells in addition to generating more side effects. CNTs as drug delivery vehicles have shown potential in targeting specific cancer cells with a dosage lower than conventional drugs used [3], that is just as effective in killing the cells, however does not harm healthy cells and significantly reduces side effects [4].

1.4 Background of research work of Carbon Nanotubes

The potential of carbon nanotubes has developed ideas in exploring their mechanical properties, deformation under loading, and as resultant from the loads applied, the possible failures of carbon nanotubes. These miniature tubes are observed to be more complex compare to many other existing materials, due to its miniature and nanoscale level size. Hence, both experimental and numerical work has been adopted for that purposes. The numerical approach can be divided into two; the molecular dynamics and continuum mechanics approach. Molecular dynamics approach is observed to have benefits in dealing with any type of problems. However, due to its high computational tasks, they limit its application to small number of atoms or molecules. Therefore, practically, its application is only for SWCNTs with small number of atoms modeling. The continuum mechanics approach is mainly concentrated on the simulation of static and dynamic properties of carbon nanotubes. The technique is highly applicable to simulate SWCNTs with large number of atoms. With extend to that, continuum mechanics approach also has the capability of simulating MWCNTs. However, this approach will neglect their atomistic properties such that the interatomic forces which will slightly affect the simulations results.

1.5 Problem Statement

SWCNT is particularly complicated for any mechanical test due to its nanoscale size. Continuum mechanics approach is applied to study the mechanical properties of carbon nanotubes. In addition, the difficulties involved in the handling of these nano-scale molecules make the findings of their mechanical properties a relatively challenging assignment.

As predicted, SWCNTs are not nearly as strong under compression because of their hollow structures and high aspect ratio. They have a tendency to undergo buckling when placed under axial loading. Hence, it is important to find and investigate the buckling behavior of the SWCNTs.

1.6 Objectives

The first objective of this final year project is to develop and implement a suitable finite element model of SWCNTs. Secondly, is to investigate the buckling behavior of SWCNTs based on the concept of continuum mechanics.

1.7 Scope of Study

With proper simulations using ANSYS software, the buckling behavior of SWCNTs is predicted based on application of axial loading. The simulation is using non-linear 188 beam element to demonstrate a non-linear deformation.

The buckling behavior is investigated on (10, 10) armchair SWCNTs with four (4) different lengths which are 5, 10, 15 and 20 nm.

The beam non-linear properties are determined using the concept of equivalence between molecular dynamics and continuum mechanics.

CHAPTER 2

LITERATURE REVIEW

As basic reference, Salvetat-Delmotte and Rubio [5] had discussed on the mechanical properties of carbon nanoutubes. Theories as well as experiments are investigated with a view for the readers to extract the fundamental of carbon nanotubes itself [5]. With simple review on the previous literatures, CNTs are observed as a great potential in reinforcing elements for composites. A Young's modulus for SWCNTs and multi wall carbon nanotubes (MWCNTs) was reported to be 1.25 TPa, at the same time as a Poisson's ratio approximately 0.14-0.28 was reported depending on the approach and the energy potential used [5].

Various experiments and simulations to determine the physical properties and electronic properties of SWCNTs are existed in the literatures [1-15], especially in the development of finite element modelling. Numerical or computational simulation for predicting mechanical properties of CNTs has been acknowledged to be a great tool to overcome the difficulties arising from the measurement of nanoscale dimensions. Subsequently, both molecular dynamics and continuum mechanics approach are adopted by scientist in order to determine the potential properties of SWCNTs.

A continuum mechanics approach has been developed for the modelling carbon nanotubes by Li and Chou [1]. The numerical modelling is based on the theory of a simple linkage between molecular mechanics and structural mechanics. In this proposed method, the computational approach is fundamentally classical structural mechanics. However, the theoretical concept is captured from modern computational chemistry and the modelling is still reserved at the atomistic scale. Li and Chou simulated the buckling behavior of CNT under compressive load and the deformation in tensile test of clamped CNTs.

Three- dimensional finite element models for armchair, zig-zag and chiral SWCNTs were developed by Tserpesa and Papanikos [2]. The model development is based on the assumptions that CNTs, when subjected to loading, behave like a space-frame structures.

The bonds between carbon atoms are considered as connecting load-carrying members, while the carbon atoms as joints of the members [2].Hence, the carbon nanotubes' carbon atoms are bonded by covalent bonds forming a hexagonal lattice. Hence, the total deformation of the carbon nanotubes is determined by the interactions between the bonds. With extend to this method; the model can be applied to investigate the behavior of SWCNTs as well as MWCNTs. Using the developed model, an investigation of the value of the Young's modulus based on different chirality, wall thickness, and diameter of the SWCNTs. The results are compared to several literatures such as [6] and [7] and are well accordingly similar.

In recent paper, Chen et al. [8] had demonstrated eigenvalue buckling analysis for armchair and zigzag SWCNTs under axial compression. The relationship between the length and diameter of the tube and the buckling mode and critical buckling load were investigated. The simulation was based on continuum mechanics approach which adapted work done by [2]. Hence, a modeling based on a beam theory is created and well-simulated the buckling behavior of SWCNTs. Results show that the critical buckling load decreases as the length of the tubes increases also as the diameter increases.

While according Meo and Rossi [6], non-linear torsional spring element is proposed based on the molecular dynamics theory. With the proposed element, Young's Modulus of C-C bond, graphene sheet and carbon nanotubes are investigated. An average of 0.915±0.008 TPa value of Young's modulus was found in good agreement with existing numerical and experimental works by various researchers [6]. Based on molecular dynamics calculations, Nardelli et al. [9] have predicted that an armchair CNT can support an axial compression strain of 0.05 before buckling. For critical stress for fracture, it is expected to be between 100 and 150 GPa for thin tubes, reported by Lourie et al. [10] and [9].

On the other hand, molecular dynamics approach was also used by Zhang and Shen [11] to determine the buckling and post-buckling behavior of SWCNTs in thermal environments via molecular dynamics simulation. Based on the inter-atomic interaction

potentials, post-buckling equilibrium paths are determined as well as the variation of energy strain. The result shows that the Van der Waals interaction for axial compression load can be negligible. Numerical results are for two types of armchair (12, 12)-tube and the zigzag (21, 10)-tube under axial compression, torsion and external pressure. The results also show that the temperature change has significant effect on the post-buckling response of SWCNTs under axial compression, but has a small effect in the loading case of torsion [11].

Based on modified structural mechanics approach, buckling behavior of SWCNTs under bending is also simulated by Wan and Delale [12]. The bonds which are the beam elements are considered having rectangular cross -section and the out-of plane deformation of the bonds are observed. The structural mechanics approach was modified and based on the work done by [1]. In addition, the proposed modified structural mechanics approach to investigate the buckling of CNTs under bending. A 7.53 nm long zigzag nanotube (17, 0) is used. Displacements boundary conditions are applied on the atoms at the end rings so that atoms at both ends remain circular and in plane perpendicular to the deformed axis throughout the deformation [12]. Onwards, the bending angle is increased in small increment to simulate large rotation. Results shows that the critical angle θ_{cr}= 22.32^{o}. The deformation is as shown as in figure 5.

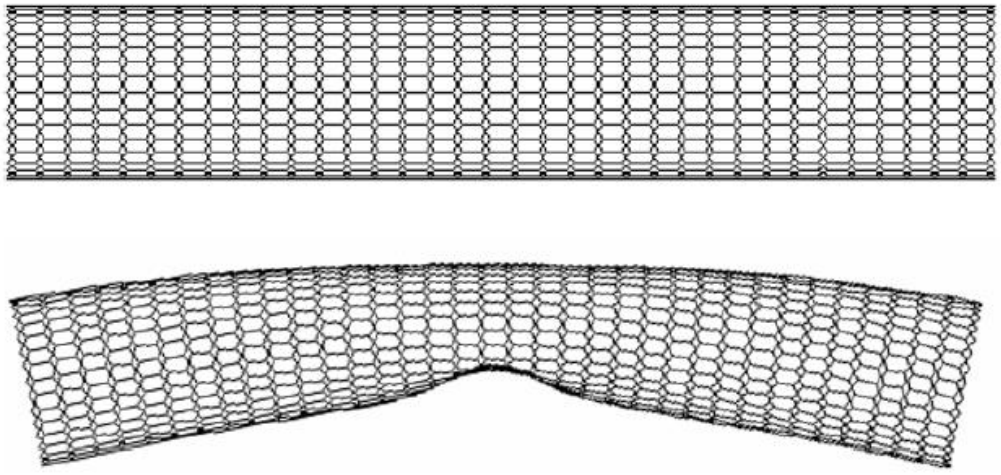

Figure 5: Bending buckling of 7.53 nm long (17, 0) CNT by [12]

Li and Chou in [1] also reported their other work in [13] that the elastic buckling behavior of carbon nanotubes where both axial compression and bending loading are considered. The same approach used by their previous work in [1] and also work done by [2]. The effects of nanotube diameter, aspect ratio, and tube chirality on the buckling behavior are investigated. The results show that the buckling forces decrease in increase of nanotube aspect ratio.

The buckling phenomena of armchair nanotubes under axial compression, bending and torsion for instance were modeled by Yakobson et al. [7] and Chen et al.[8] using classical Brenner potential in their molecular dynamics simulation. The result reveals that the temperature changes will influence the post-buckling behavior of nanotubes. Since molecular dynamics method is well suited with smaller nanotubes, an armchair SWCNT with length of 6 nm and diameter of 1 nm is simulated. The molecular results are then compared with the existing findings in continuum mechanics approach.

In conjunction with both method described above, as prepared by E. Mohammadpour, M. Awang et al. [14], a finite element simulation technique for estimating the mechanical properties of Single-Walled Carbon Nanotube (SWCNT), polymer composite is developed [14]. Their work is using the same approach like [1] where the individual carbon nanotube is simulated as a frame-like structure and the primary bonds between the two nearest-neighboring atoms are treated as 3D beam elements. The beam element non-linear properties are determined using the concept of energy equivalence between molecular dynamics and structural mechanics with Modified Morse potential as per presented by Meo and Rossi [6].

Hence, the Young's modulus of SWCNTs is estimated to show the accuracy of this simulation method. Results from their work showed that the obtained mechanical properties of nanotubes by the present method are in good agreement with several comparable numerical and experimental results such as [2] and [6]. Moreover, the relations between the mechanical properties and the nanotube size are also investigated to give a better understanding of the variation of mechanical properties of nanotubes.

Using finite element method E. Mohammadpour and M. Awang [15] has also predicted a stretching behavior of carbon nanotubes. The method is simplified based on the theory proposed by [2] and [6]. The tensile properties obtained for this work is the Young's modulus and tensile failure. Specifically, non-linear beam element is demonstrated and using the finite element model, Young's modulus for (10, 10) SWCNTs are calculated for different values of thickness which are 1.47 Å and 3.4 Å. The results show values and curve which adapted the same curve by [6].

CHAPTER 3

METHODOLOGY

3.1 Background of SWCNTs simulation for buckling analysis

The background of the simulation is based on two approaches; the molecular mechanics approach and continuum (structural) mechanics approach. The molecular mechanics approach is based on the chemical bonding in the SWCNTs while the continuum mechanics approach is based on the structural mechanics properties of the SWCNTs.

In this work, the continuum mechanics model of SWCNTs was developed based on the model proposed by Tserpes and Papanikos [2]. In continuum mechanics method, the SWCNT is viewed as a structure consists of nodes connected by beam elements. One node represents one carbon atom, while the beam element acted as a covalent bond. This configuration is called as a space-frame structure as shown in figure 6.

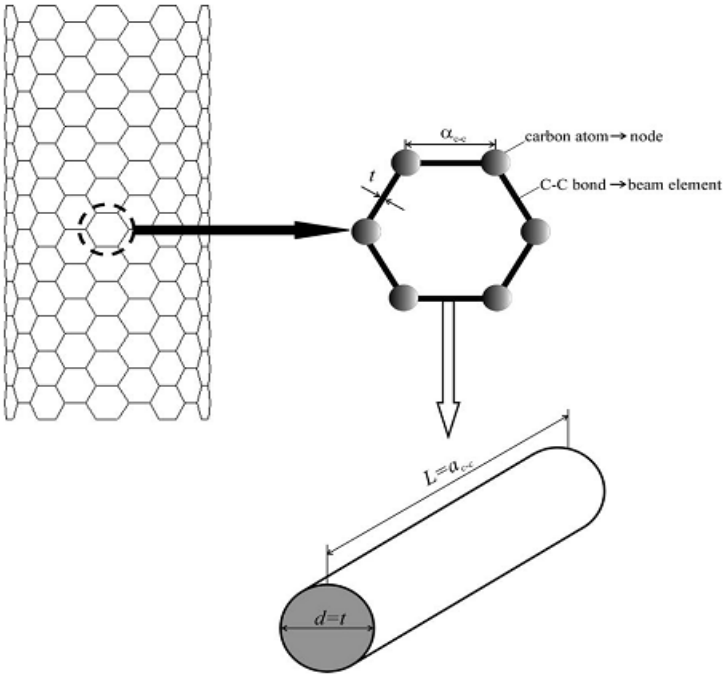

Figure 6: Model of a SWCNT as a space-frame structure [2]

The beam non-linear properties are determined using the concept of equivalence between molecular dynamics and continuum mechanics based on Modified Morse potential. Some examples of the reactions are shown in figure 7.

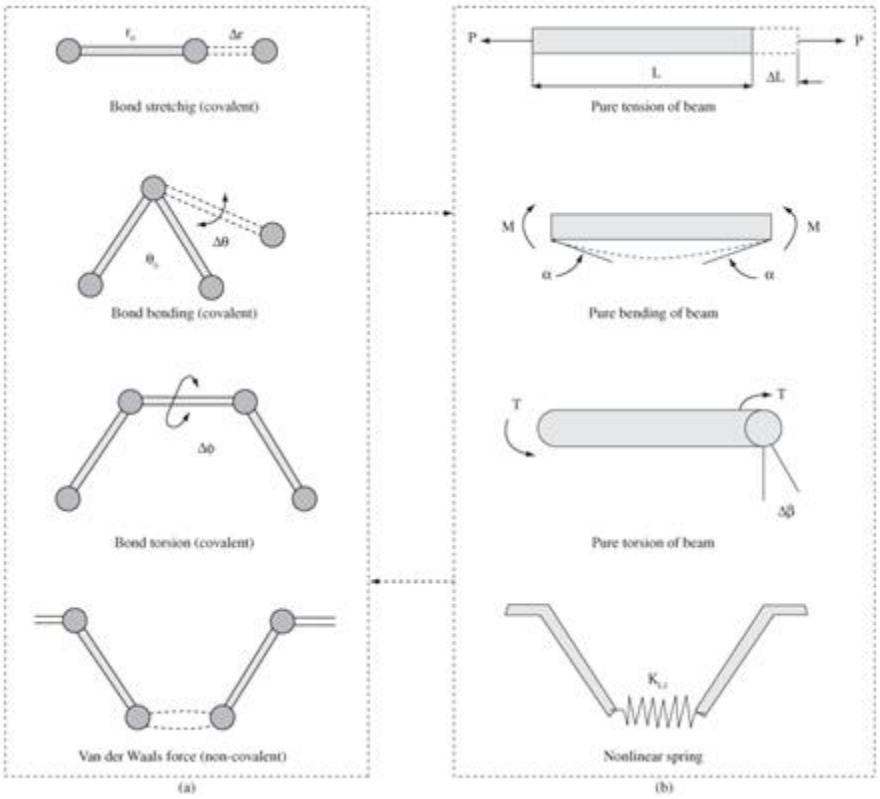

Figure 7: Example of some equivalent between molecular dynamics and continuum mechanics approach a) molecular dynamics b) continuum mechanics

According to [6], in order to determine the SWCNT mechanical properties, the molecular dynamics theory can be applied. Since the carbon nanotube is viewed as molecules with carbon atoms bonded with covalent bonds, the general expression of the potential energy is the summation the bonded and non-bonded interactions as below. The force field being generated being generated from this potential function and acting on the moving nuclei is called the molecular force field [6]. In its general formula, the potential energy is described as:

$$U_{total} = \sum U_r + \sum U_\theta + \sum U_\emptyset + \sum U_\omega + \sum U_{vdw} + \sum U_{el} \qquad (1)$$

Where U_r is the bond stretching, U_θ is the bond angle bending, $U_\emptyset$ is the dihedral angle torsion, U_ω is the inversion terms, U_{vdw} is the Van der Walls interaction and U_{el} is the electrostatic interaction.

Fundamentally, in the model of bond stretching (figure 8), a simple analytical Morse function is used to represent the bond energy curve.

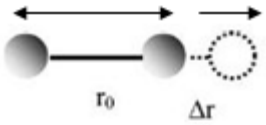

Figure 8: Schematic diagram of bond stretching

$$U_r = D_e \left\{ \left[1 - e^{-\beta(r-r_0)} \right]^2 - 1 \right\} \tag{2}$$

r_0 is the bond equilibrium length, D_e is the dissociation energy and β is a fitting parameter. The following parameters were used in [6] and [15] as well as in this work: $r_0 = 0.139\ nm, D_e = 6.03105 \times 10^{-10} N.nm, \beta = 2.625 \times 10^{10}\ m^{-1} = 26.25\ nm^{-1}$.

In structural mechanics approach, U_r is define as the stretching energy of a bond and the equation is

$$U_r = \frac{1}{2}\ k_r (r - r_0)^2 = \frac{1}{2} k_r (\Delta r)^2 \tag{3}$$

k_r is the bond stretching constant, while Δr represents the bond stretching increment. Apparently, it can be concluded that the U_r and U_A signify the stretching energy in both of the approaches, molecular dynamics and continuum mechanics.

According to the continuum mechanics, the strain is energy of a beam with given length, L and cross-section, A can be expressed as

$$U_A = \frac{1}{2} \int_0^L \frac{N^2}{EA}\ dL = \frac{1}{2}\ \frac{N^2 L}{EA} = \frac{1}{2}\ \frac{EA}{L}\ (\Delta L)^2 \tag{4}$$

By comparing the molecular and structural mechanics equations,

$$U_A = U_r$$

$$\frac{1}{2}k_r(\Delta r)^2 = \frac{1}{2}\frac{EA}{L}(\Delta L)^2;\ \Delta r = \Delta L \tag{5}$$

where ΔL is the stretching deformation of the beam. Therefore,

$$\frac{EA}{L} = k_r; A = \frac{\pi d^2}{4}$$

$$k_r = \frac{E\pi d^2}{4L} \tag{6}$$

Thus, from here, the diameter of the beam is determined as well as the cross sectional area of the element which represents the bond of C-C atoms.

One of the benefits of finite element method is by substituting the carbon nanotubes with an equivalent structural modelling; it is not only can determine the mechanical properties of CNTs but also can simulate behavior of CNT under various types of loads.

Based on this concept, a model of carbon-carbon atom is model using a non-linear beam element is modeled. The equivalence of molecular mechanics approach and structural mechanics approach is used to determine the beam element non-linear properties. The model is built using the finite element commercial code ANSYS. The type of beam used is BEAM188. This is due to its ability to simulate a non-linear deformation of the structure.

By deriving the Morse potential for bond stretching, the relationship of force and the displacement of the bond can be determined. Hence, the material properties of the non-linear beam are acquired.

$$F(\Delta r) = 2\beta D_e\left(1 - e^{-\beta\Delta r}\right)e^{-\beta\Delta r} \tag{7}$$

From above derived equation, a curve is plot as figure 9 to view the stretching behavior of the covalent bond.

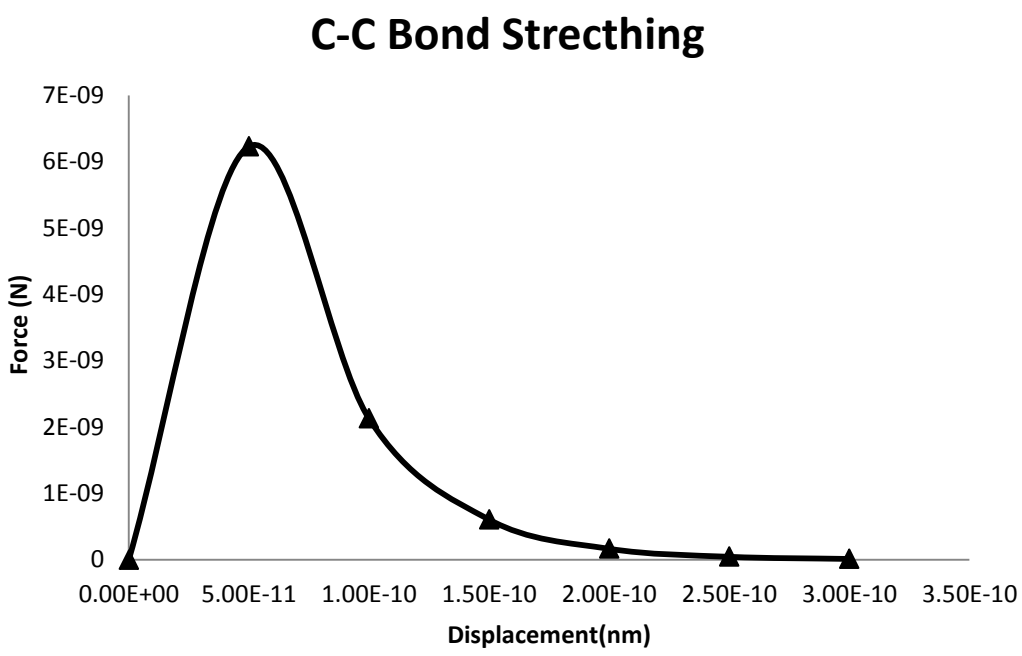

Figure 9: Force vs displacement curve based on Morse potential

3.2 Finite Element Modelling

Based on continuum mechanics theory mentioned, a model of carbon-carbon atom is model using a non-linear beam element is modeled. The equivalence of molecular mechanics approach and structural mechanics approach is used to determine the beam element non-linear properties. The model is built using the finite element commercial code ANSYS. In the modelling work, there are four (4) main modules based on the theories as describe is Figure 10 below.

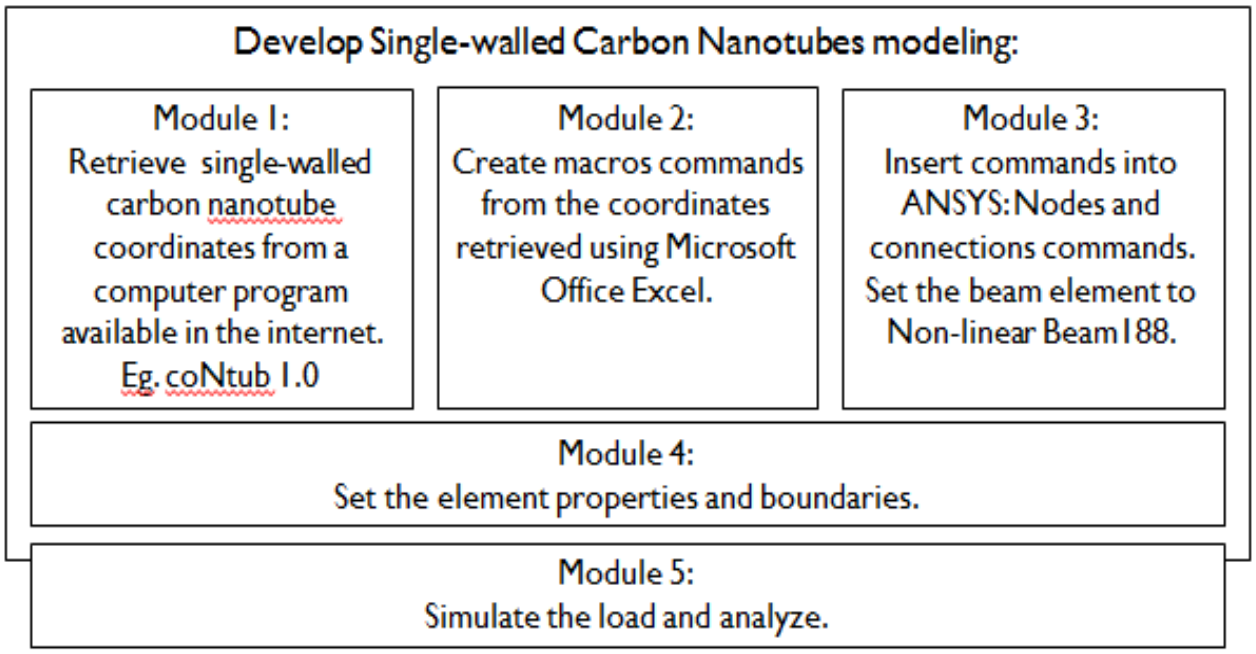

Figure 10: Modelling method of buckling analysis of SWCNT

3.2.1 SWCNT model

The coordinates retrieved from the coNtub v1.0 program is inserted into some macros command in Microsoft Excel and these coordinates will be divided into two parts which are the nodes and elements. Insert coding method is used, the model the structure such that will illustrate the real SWCNT structure as shown in Figure 11 and 12.

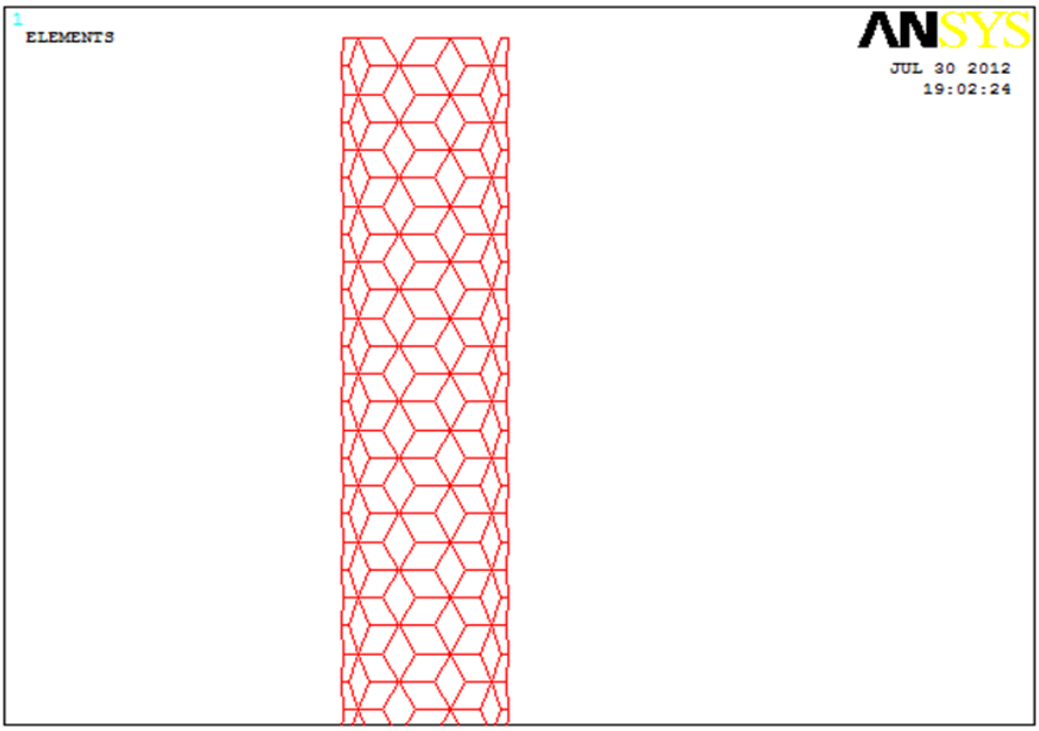

Figure 11: Meshed model of armchair (10, 10) SWCNT

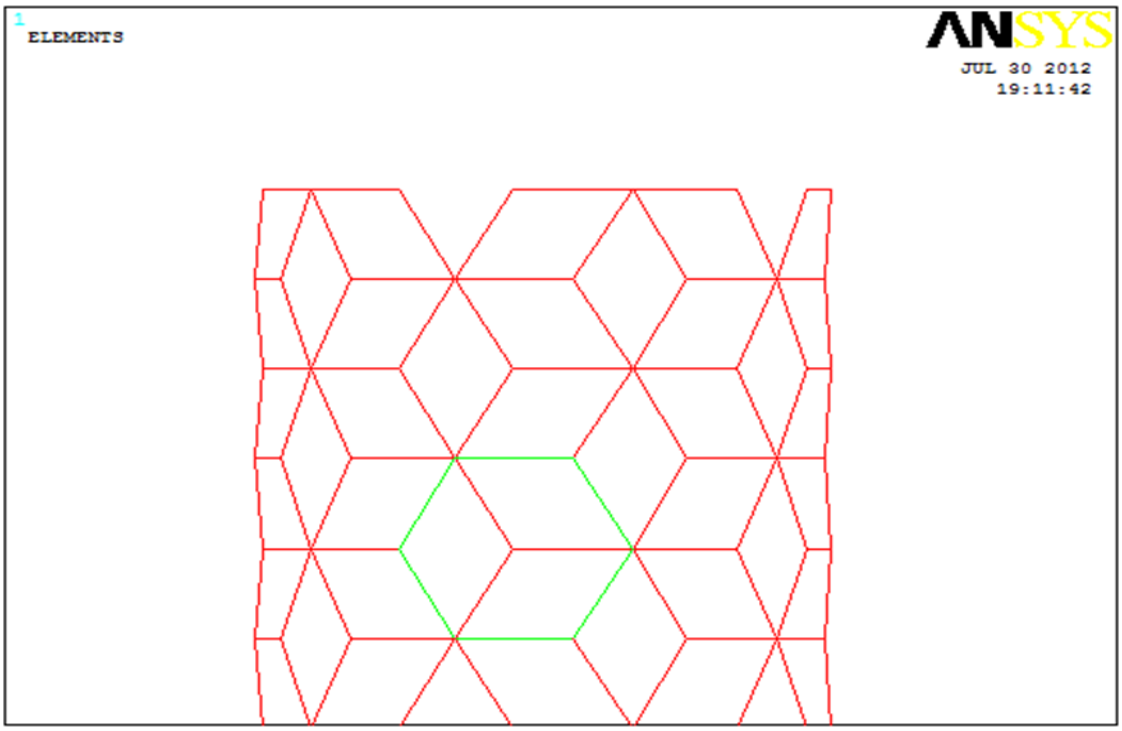

Figure 12: Hexagonal structure of SWCNT

3.2.2 Element Type

The element type used in this work is BEAM188. This element is well- suited for linear, large rotation, and / or large strain non-linear applications. BEAM188 is also recommended since it is easy to use both in pre-processing and post-processing phase.

It has six (6) degrees of freedom which are; translations in the x, y and z directions and rotations about the x, y and z directions. Another seventh degree of freedom which is the warping magnitude is optional.

The defined cross-section value is circular of 7.35 nm diameter and the DOFs are defined in global cylindrical coordinate system.

3.2.3 Material Properties

In ANSYS, the element is defined as BEAM188 element with initial stiffness, cross sectional area, multi-linear isotropic hardening material properties (MISO) and isotropic linear material properties. For the isotropic linear properties, the initial stiffness value is 6.719×10^{12} and the poisson ratio is defined as 0.3 based on existing literatures [2, 6].Based on the force vs displacement curve discussed in the previous subtopic (figure 9) and equation 8, another curve is constructed to define MISO as shown in figure 8 and 9. The curve consists of twenty (20) points defined (figure 13 and 14), which are the stress and strain values. These values are inserted to ANSYS via coding method.

$$\sigma = \frac{F}{A} \; and \; \varepsilon = \frac{\delta}{L_0} \tag{8}$$

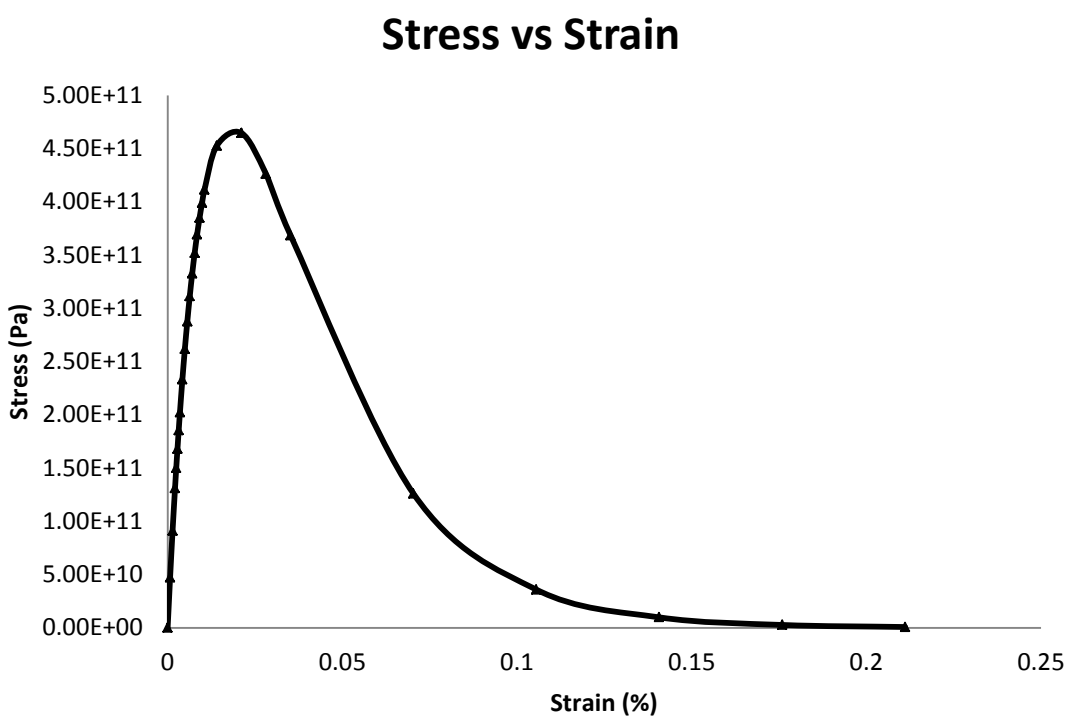

Figure 13: Stress vs strain curve based on Morse potential

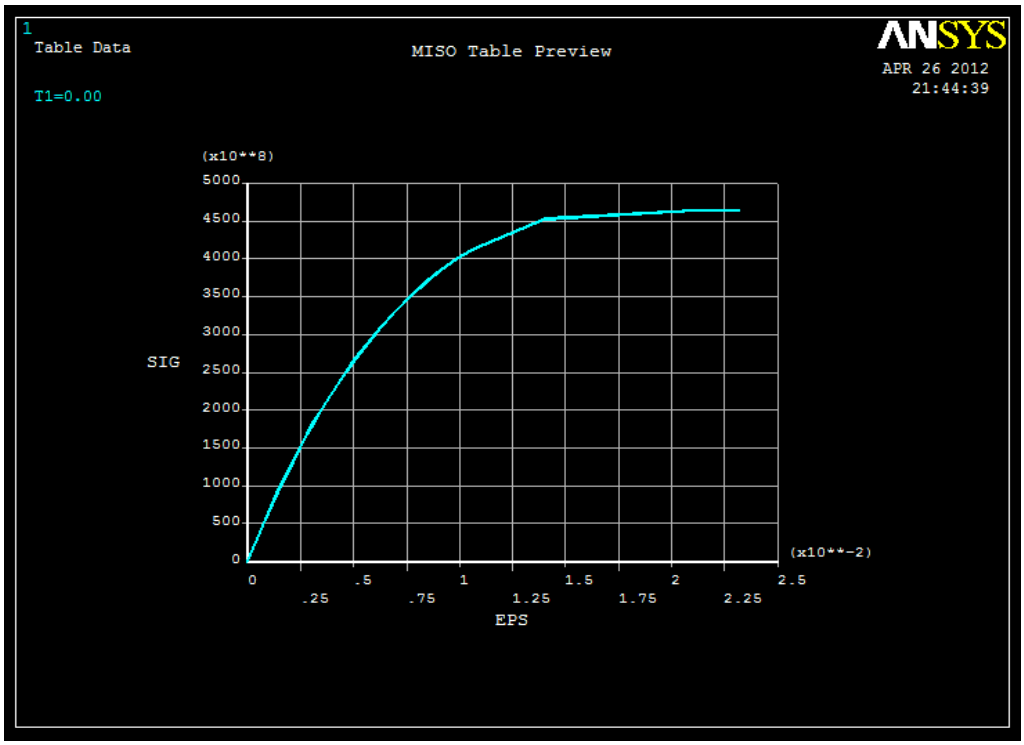

Figure 14: MISO curve preview

3.2.4 Boundary Conditions

Figure 15 and 16 shows the applied boundary conditions. At bottom end of the SWCNT, all six (6) degree of freedoms (DOFs) are constrained which means to be fixed. At the top end of the tube, all of the DOFs are constrained; except for the translation of z. Well-distributed negative loads will be applied to the unconstrained DOFs at the top of the tube. The same boundary conditions are applied based on work done by [8] but with a non-linear beam elements.

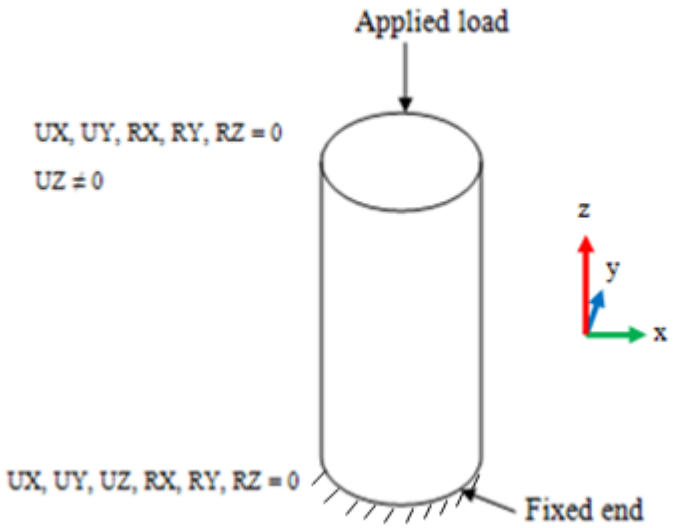

Figure 15: Schematic diagram of boundary conditions applied for buckling analysis

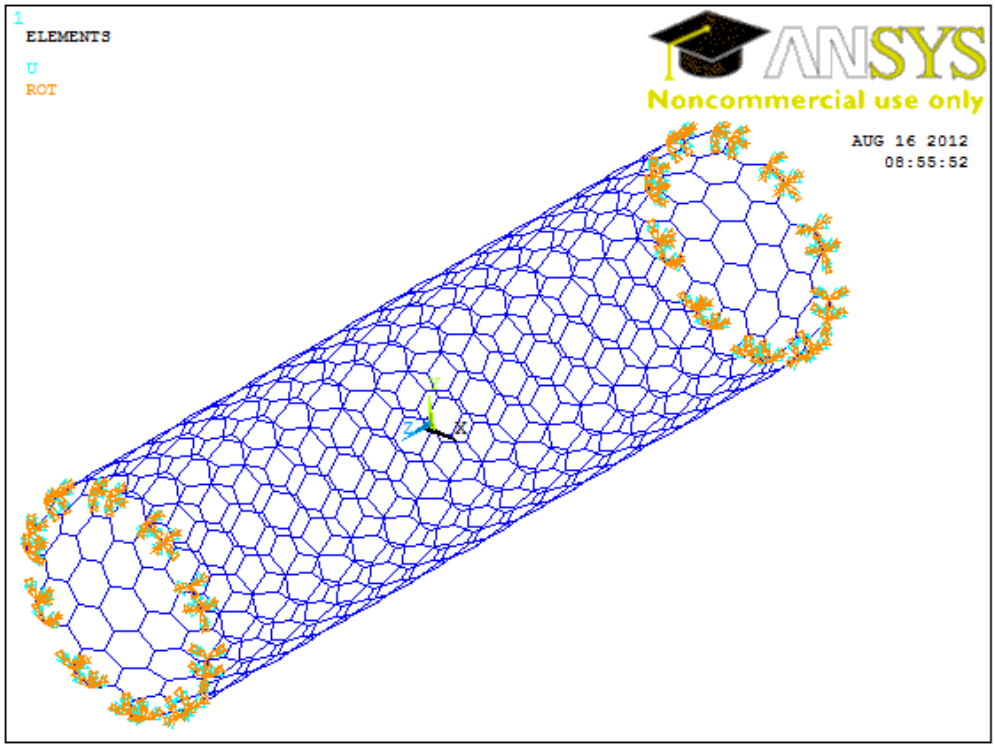

Figure 16: Boundary conditions for SWCNT buckling analysis as shown in ANSYS

3.3 Method Verification

Young's modulus of SWCNTs was investigated to verify of the simulation method proposed by [14] and [15]. Moreover, the relations between the mechanical properties and the nanotube size are also investigated to give a better understanding of the variation of mechanical properties of nanotubes. Stretching displacement is applied at the top end of the tube to study the tensile stretching behavior of the tube.

To verify the method proposed, a (5, 5) armchair SWCNT was modeled and simulated. The length used was 10 nm which the number of nodes is 810 and the number of elements is 1,200. Stretching displacement is applied at the top end of the tube to study the tensile stretching behavior of the tube.

The nanotube Young's modulus is evaluated with equation obtained from the equation 9. F is the reaction force of the displacement of the SWCNT, L is the original length of the

SWCNT, A is the cross section area of the SWCNT and ΔL is the displacement applied on the SWCNT.

$$E = \frac{\sigma}{\varepsilon} = \frac{FL}{A\Delta L} \tag{9}$$

The cross section area and diameter of the tube can be defined from the chirality of the SWCNT based on equation 10 and 11. The value of a_0 is equal to 0.142 nm.

$$A = \pi D_n t_n \tag{10}$$

$$D = \frac{a_0\sqrt{3(n^2+m^2+mn)}}{4\pi} \tag{11}$$

The bottom end is fixed and the structure is will be displaced positive at the top in translation z direction as to simulate the axial stretching displacement as shown in figure 17 and 18.

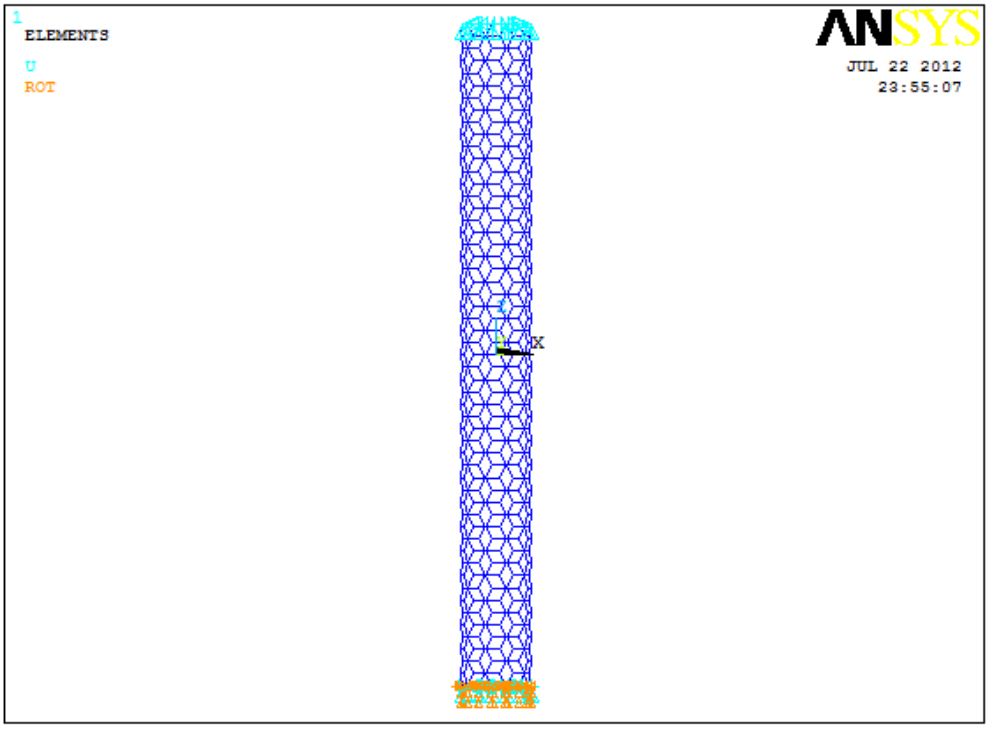

Figure 17: Boundary condition for stretching of armchair SWCNT (5, 5)

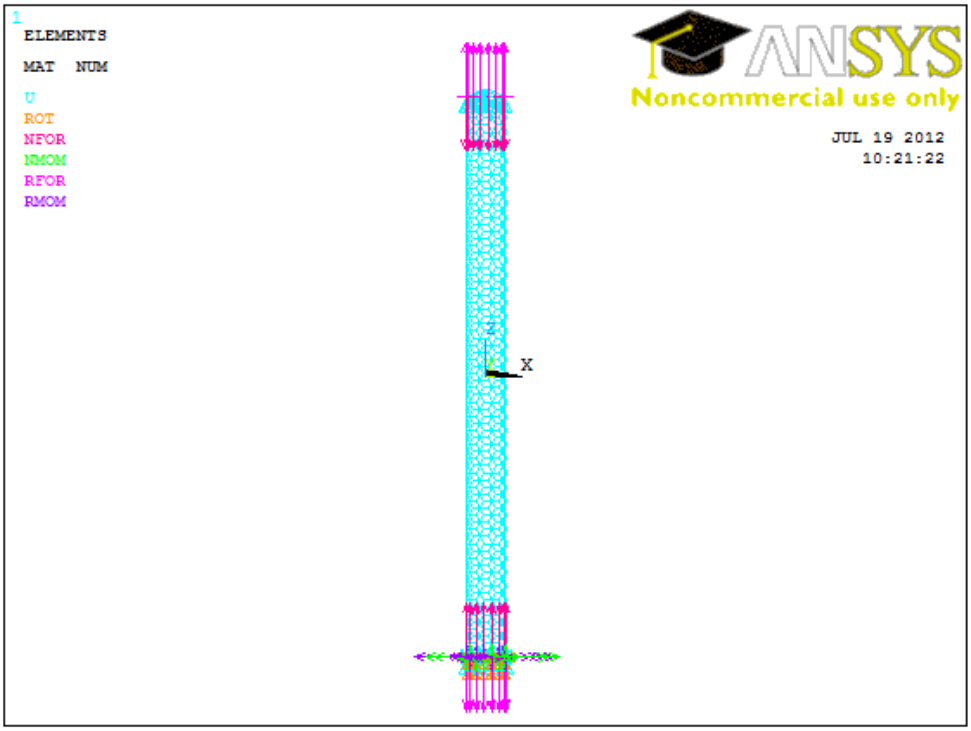

Figure 18: Reactions and boundary conditions applied for stretching of armchair SWCNT (5, 5)

3.4 Key Milestone and Gantt Chart

No.	Detail/Week	1	2	3	4	5	6	7		8	9	10	11	12	13	14	
FYP 1																	
1	Literature Review and Introduction to CNT								Mid- Semester Break								Semester Break
3	ANSYS Tutorial																
4	Study of Molecular Dynamics and Structural Mechanics Method																
5	Extended Proposal Submission																
6	Modelling of SWCNT Tutorial																
7	Preparation of Proposal Defence Presentation																
8	Proposal Defence Presentation																
9	Modelling via coNtube 1.0 for coordinates retrieval																
10	Interim Report Submission (draft)																
11	Commencement of Modelling																

	of SWCNT																
12	Interim Report submission																
No.	Detail/Week	1	2	3	4	5	6	7		8	9	10	11	12	13	14	
FYP 2																	
1	Continue Modelling								Mid- Semester Break								Semester Break
2	Load and Pressure Simulation																
3	Submission of Progress Report																
4	Solving and deformation analysis																
5	Pre-EDX																
6	Submission of draft report																
7	Project VIVA																
8	Final Report, dissertation compilation and submission																

CHAPTER 4

RESULTS AND DISCUSSIONS

4.1 Method verification results

The deformed mode of stretching of a SWCNT is shown in figure 19. Upon the stretching, the atoms at the top of the tube are displaced in the positive z translation DOF. Hence, the tensile or stretching modulus of the structure can be calculated.

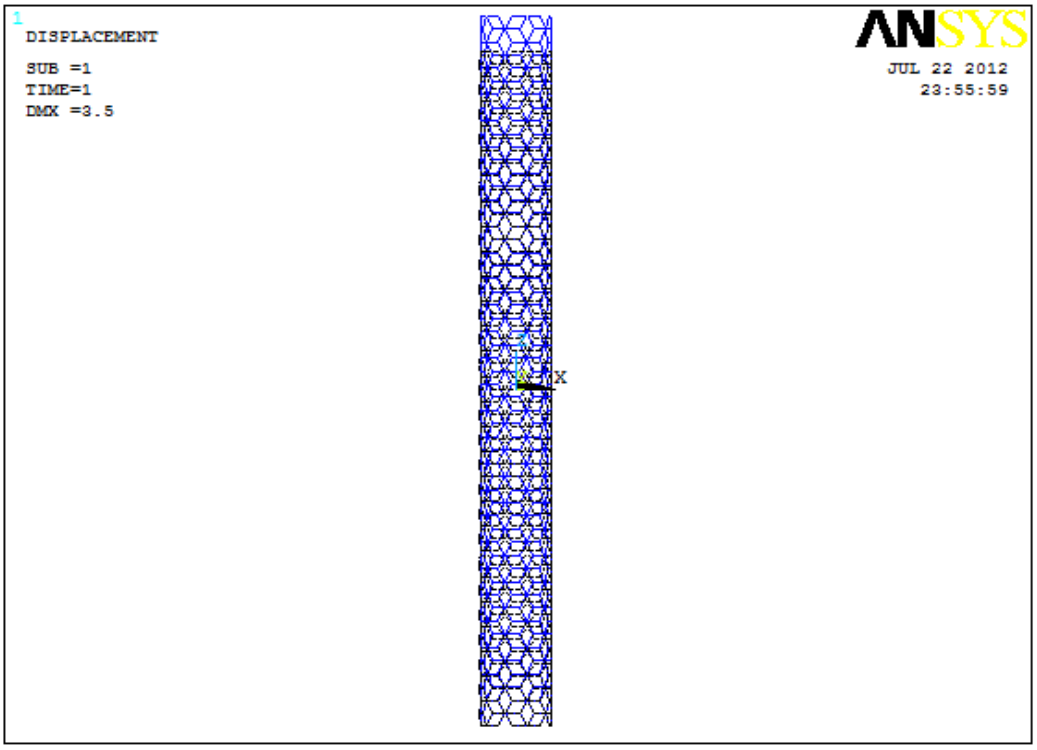

Figure 19: Stretching deformation of armchair SWCNT (5, 5)

The nanotube Young's modulus is evaluated with equation obtained from the equation 10.

$$E = \frac{\sigma}{\varepsilon} = \frac{FL}{A\Delta L} \tag{10}$$

Results showed that the obtained mechanical properties of nanotubes by the present method are in good agreement with several comparable numerical and experimental results as well as work done by [14] and [15]. The comparison of the results of present method with several other literatures is as per table 1.

Table 1: Comparison of Young's Modulus of present method with other literatures

Researcher	SWCNT Chilarity	Tube Thickness (A)	Young's Modulus (Tpa)
Present work	**(5,5)**	**3.4**	**0.873**
[2]	-	1.47	2.377
[15]	(10,10)	3.4	0.881
[6]	(10,10)	3.4	0.920

Due to the reliability of the results, work involve the analysis of buckling behavior of SWCNTs is conducted. Further, as expected, this method is also reliable in investigating the MWCNTs properties in the future.

4.2 Buckling analysis

Due to certain errors in simulations, the results obtained are adequate enough just to show the buckling behavior of the SWCNTs. One factor which is considered to have high impact in the errors is the method used in non-linear analysis.

Mostly, ANSYS used “Newton -Rhapson” approach to solve non-linear problems. In this approach, the load is subdivided into a series of load increments. The load increments can be applied to several load steps. The iterative of this method continues until the solution converges. Nevertheless, if the solution is not converged enough, several convergence recovery features can be activated to solve the problem. They are such as the line search, automatic load stepping and bisection.

The “Newton-Rhapson” approach is observed to be suitable for stretching and compressive behavior hence this method is adapted for this work. After several simulations, several errors are encountered which mostly related to the error in element formulation.

However, the results are obtained by pick in the last converged solution. Results retrieved are used to investigate the modes shown as figures 20 to 23. The buckling behaviors have significant comparison to each other due to the dislocation of certain atoms of the structure.

The simulation demonstrate the (10, 10) armchair SWCNTs with four (4) different lengths. The diameter of (10, 10) armchair SWCNT is 13.541 Å. As the length of the same tube increases, the aspect ratio (the length to diameter ratio) will increase. The trend of the analysis is predicted using axial buckling loads. The non-linear buckling analysis mode will increase the applied load until the load value causes the tube buckle sideways.

From Figure 20 to 23, the nanotube's length is proven to have significant effect on the buckling behavior. The result shows that, the atoms are dislocated and maximum displacement is observed at certain atoms of the tubes. Significantly, the displacement of the tube is observed in z and x translations directions. With proper view, the x-translation displacement is taken into account as to show the sideways buckling deformation for each SWCNT. For instance, for length of 10 nm, the SWCNT is viewed to deform sideways when the actual buckling load is applied to the structure. Hence, a SWCNT is having a potential to buckle at certain strain and stress. The atoms in the center of the tubes deformed slightly to the bottom pane and curved downwards.

With the variations of the length of the SWCNTs, the deformation is viewed to be more obvious for longer SWCNTs. the buckling modes show that the shorter tube, in this case the 5 nm length tube, is having the stiffest structure. Whereby, more loads are needed in order to make the atoms in the center buckles sideways. A more accurate iteration is observed for 10 and 20 nm length tubes which resultant in a more relevant buckling mode. From these two lengths, the deformation is viewed to be unsymmetrical and concentrated in the x-translation direction.

Moreover, the tubes are in perfect structure, without any imperfections or defects in the structure. Hence, with high tensile and compressive strength, even in buckling situation,

the bonds of the SWCNTs are not damaged. Thus, the compatibility of CNTs under large strain and stress are verified as mentioned [5].

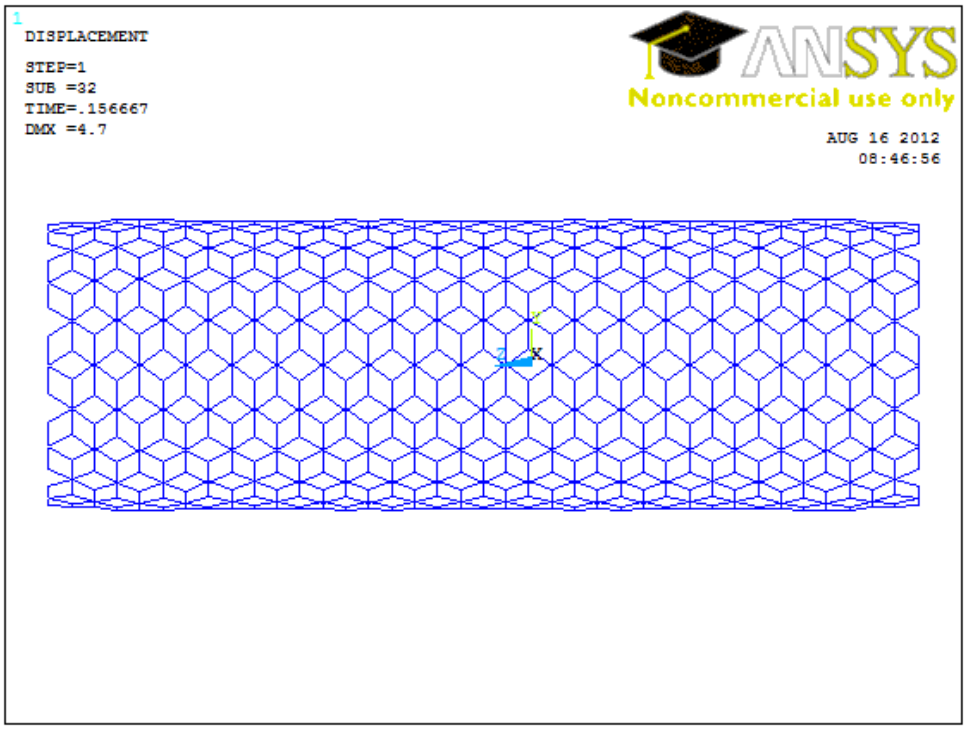

a)

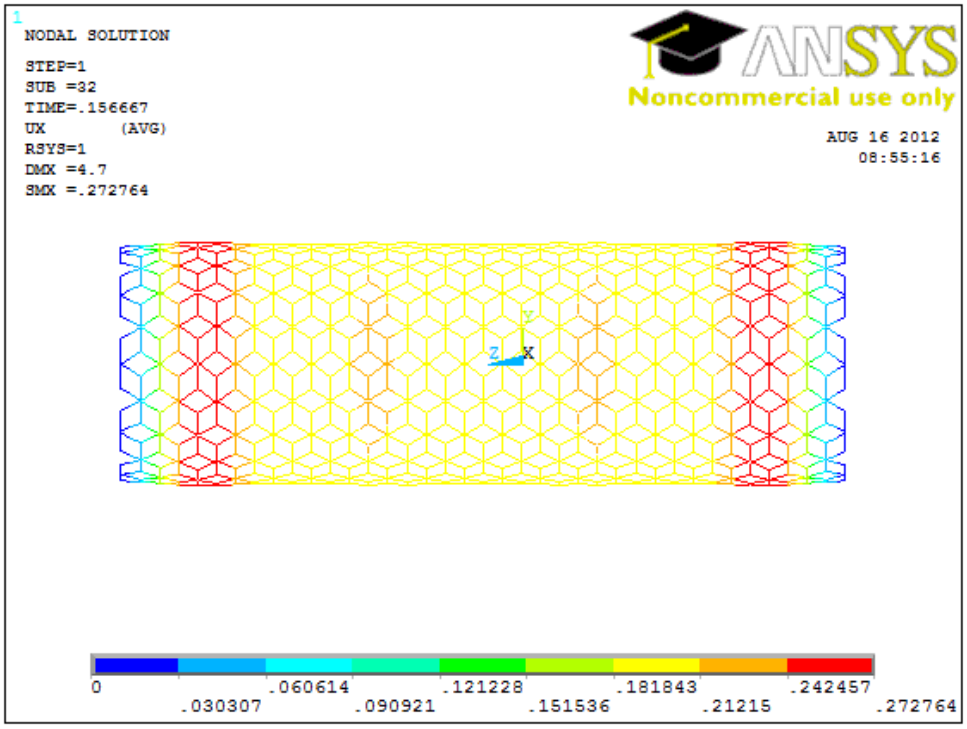

b)

Figure 20: Deformation of armchair (5, 5) of 5 nm length a) deformed mode b) nodal solution

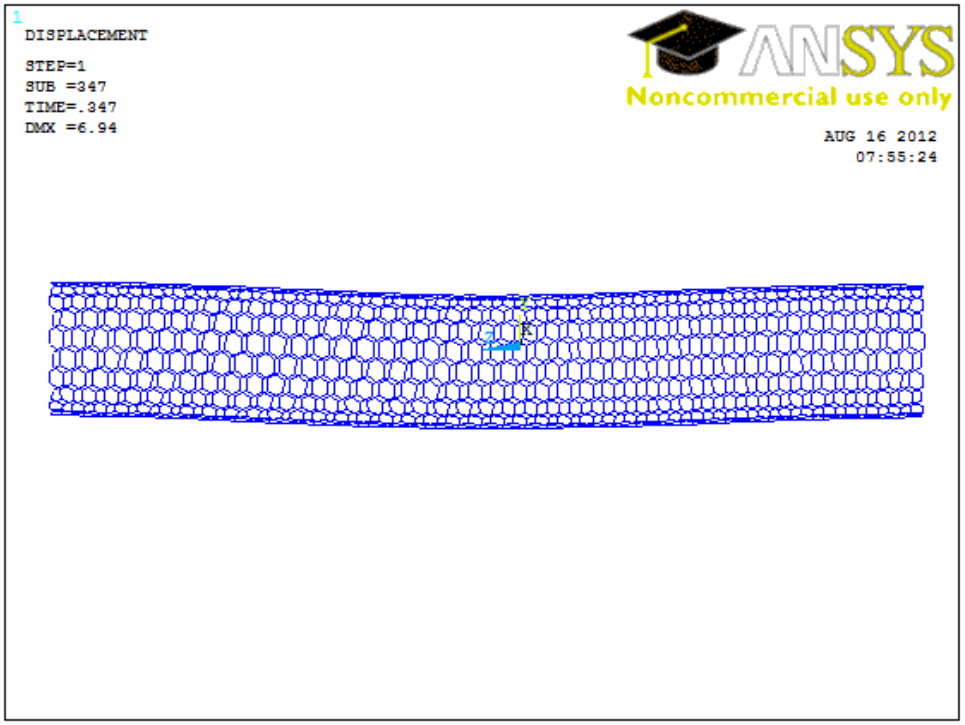

a)

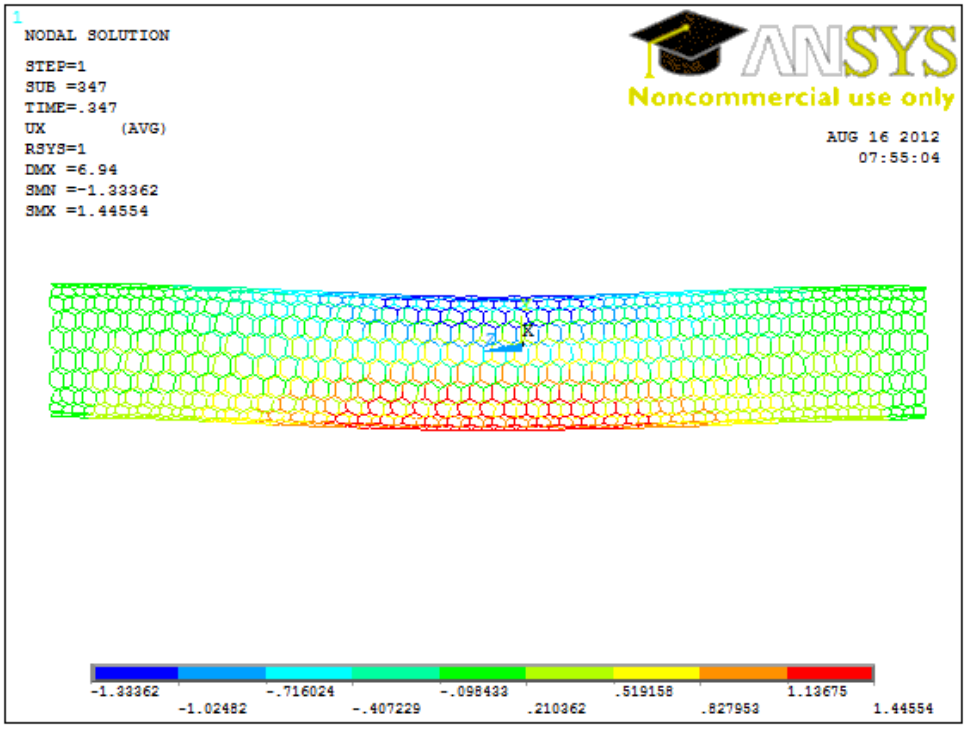

b)

Figure 21: Deformation of armchair (5, 5) of 10 nm length a) deformed mode b) nodal solution

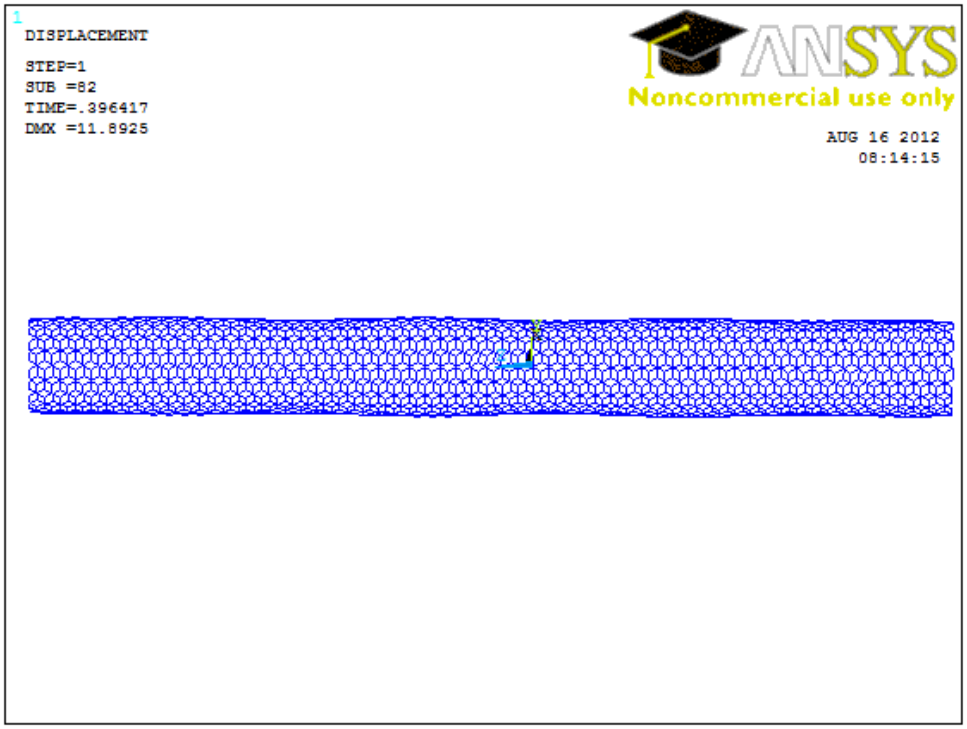

a)

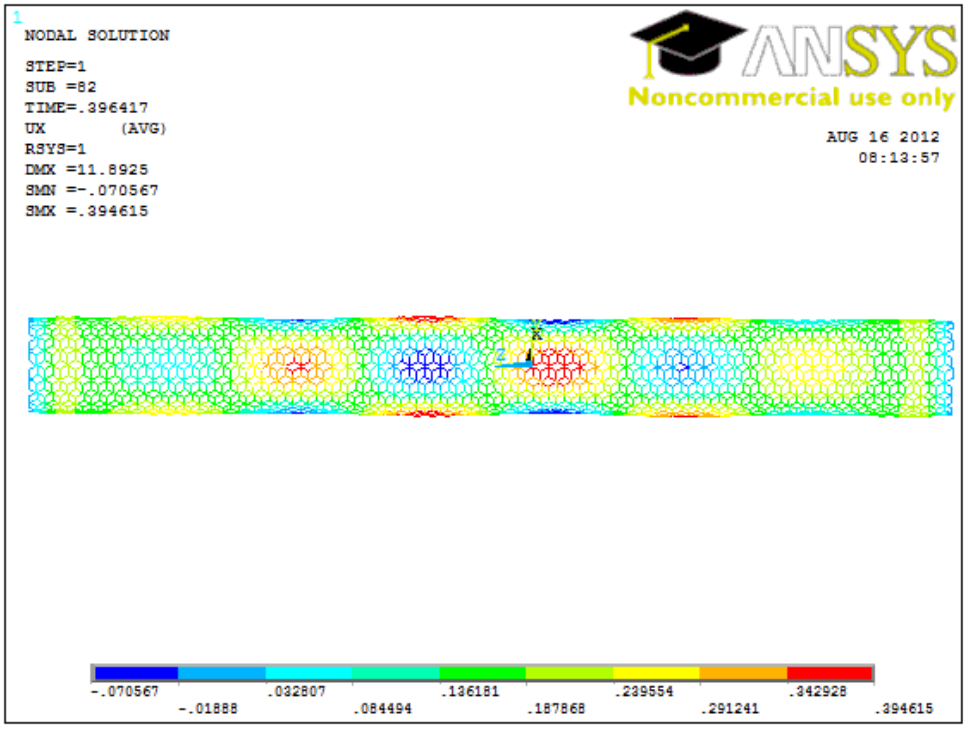

b)

Figure 22: Deformation of armchair (5, 5) of 15 nm length a) deformed mode b) nodal solution

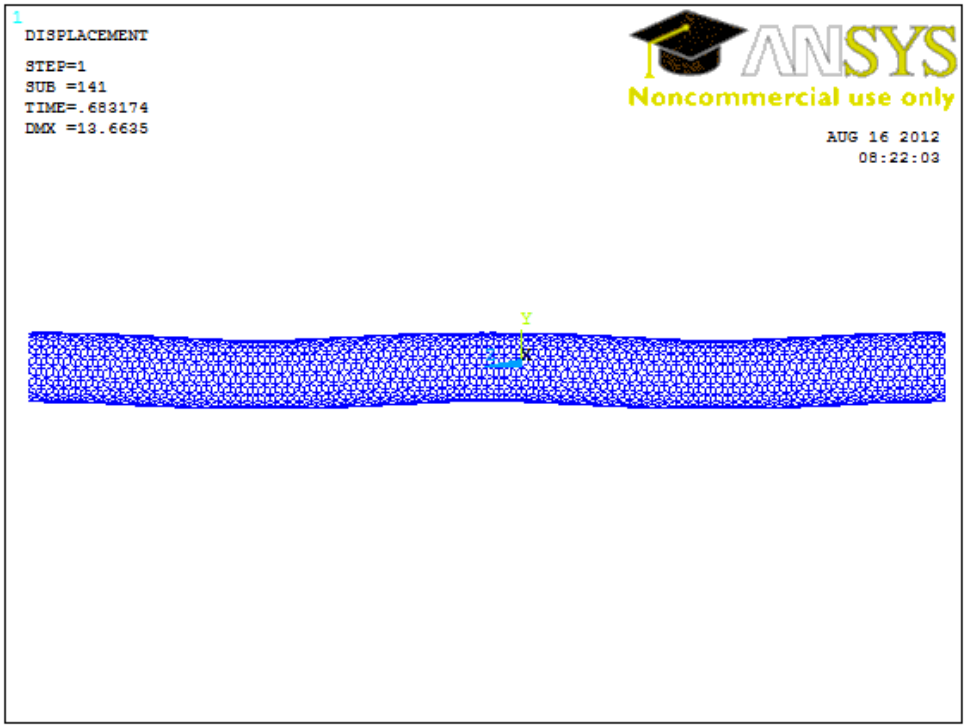

a)

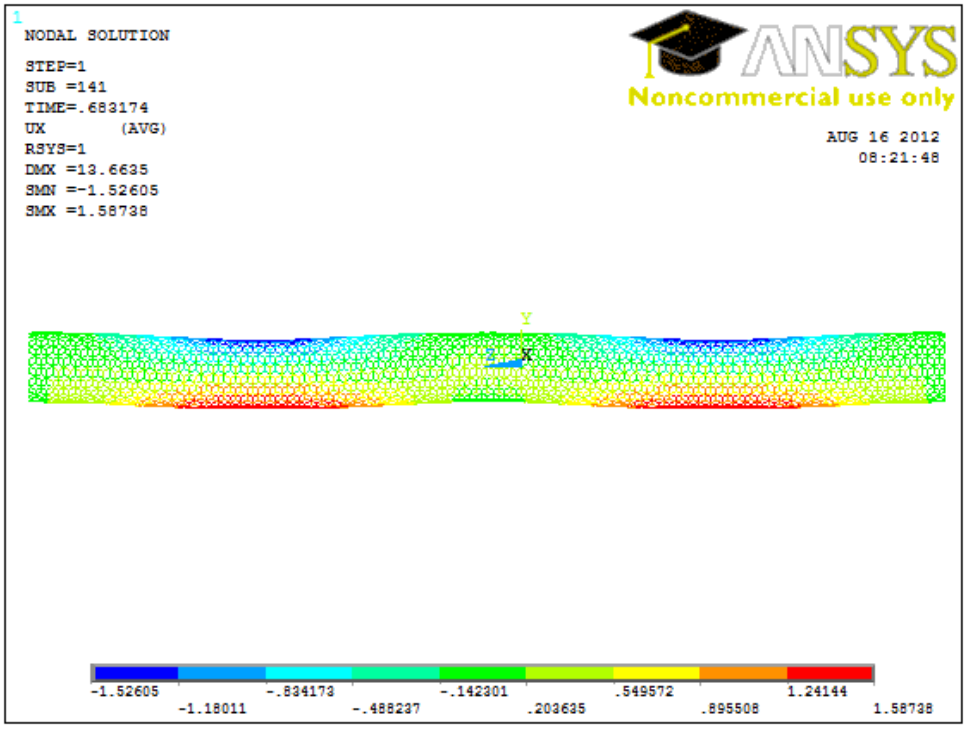

b)

Figure 23: Deformation of armchair (5, 5) of 20 nm length a) deformed mode b) nodal solution

With the length varying from 5 to 20 nm, the effect of buckling load is observed to differ. The buckling load decreases as the length of the tube increases. Thus, the results show the same trend observed by [8]. From 5 nm to 10 nm length, the load is observed having a rapid decreasing with decrement of 11% from 108 nN to 96 nN. Meanwhile, from 10 nm to 15 nm length, the do not show significant drop, with decrement of 6.2 % from 96 nN to 90 nN. The slope of the curve from 15 nm of tube length to 20 nm shows that there is a larger drop point with decrement of 16% of 90 nN. The curve of load vs length is shown in figure 24.

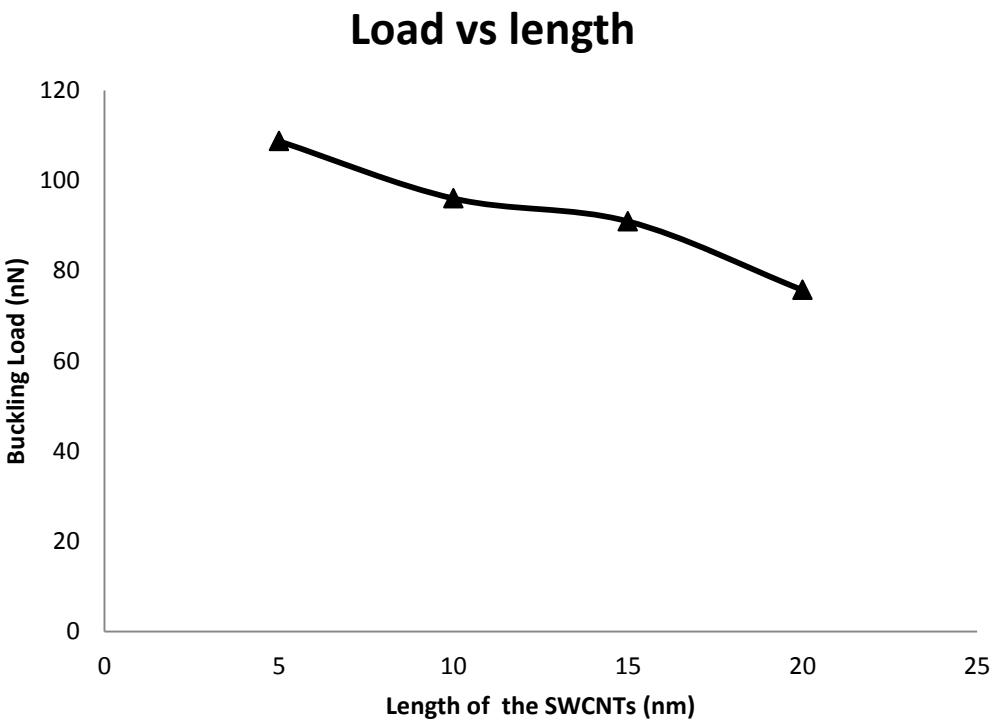

Figure 24: The relationship between the length of SWCNT and the buckling load of (10, 10) armchair SWCNT

Consequently, another relationship between the aspect ratio of the tubes and the buckling loads is investigated. Figure 25 shows that the buckling load decreases in increases of SWCNTs aspect ratio as investigated and stated by [13]. Aspect ratio is defined as the ratio of the length to the diameter of the tube. For similar chirality, the diameter is similar; hence the aspect ratio is differed by the length of the tube. Thus, the aspect ratio of longer tubes is higher.

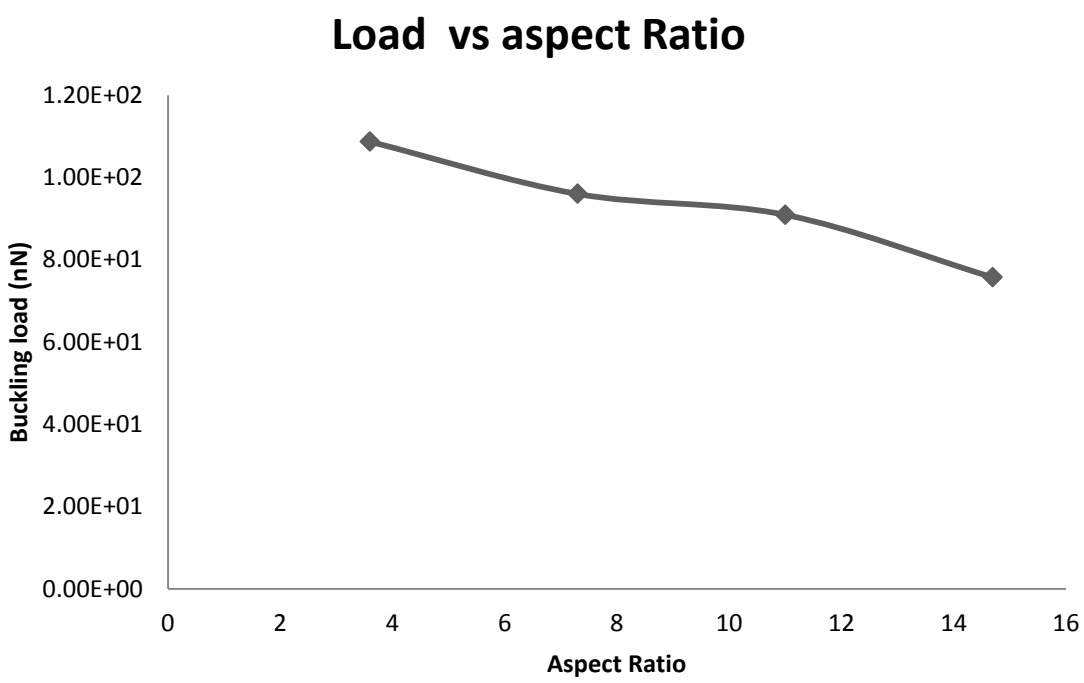

Figure 25: The relationship between the aspect ratio of SWCNT and the buckling load of (10, 10) armchair SWCNT

CHAPTER 5

CONCLUSIONS

A finite element simulation technique for SWNTs is developed which can be easily performed by commercial code ANSYS. The concept of the modelling is that molecular bonds between carbon atoms are presented as beam elements. I proposed and verified via literature a simplifying method to model non-linear nature of covalent bond between the carbon atoms of a carbon nanotube. This finite element analysis can significantly save the modelling and computing effort when it is performed. From the results in the method verification section and the outstanding benefit that the present modelling done by E. Mohammadpour, M. Awang [14,15], the concept be easily proposed to the project work which is to investigate the buckling behavior of a SWCNT.

With the length varying from 5 to 20 nm, the effect of buckling mode is observed. The critical buckling load decreases as the length of the tube increases. The results show the same trend observed by [13]. From 5 nm to 20 nm length, the load is observed having a rapid decreasing with decrement of 30.5 % from 108 nN to 75 nN. The buckling mode for every tube length has showed a significant maximum displacement in atoms of the SWCNTs.

Another conclusion, by adapting “Newton-Rhapson” method alone, the model may face several severe convergence difficulties. Such incidences include non-linear buckling analysis in which the structure collapses completely. Subsequently, the “Newton-Rhapson” method alone is not appropriate to be used. Thus, another method which is the arc-length method in cooperated along with “Newton-Rhapson” method is often used to help the problem. The arc-length method will help the “Newton-Rhapson” method iterations to converge along an arc hence preventing from divergence or error in element formulation.

CHAPTER 6

RECOMMENDATION AND FUTURE WORKS

As for another advance type of model, the spring element is proposed replace the beam element that is currently in use now. This element is already in used by [6] and results show that more accurate findings are found. This is due to the material property of a spring, which is seen to have higher sensitivity than the beam element. Moreover, based on the commercial ANSYS coding, the spring element is easier to be modeled and have less work compare to beam element.

Another investigation in obtaining an accurate buckling behavior shall be conducted prior to this project. A proper research in the adapting arc-length method may have a significant contribution to a SWCNT buckling analysis work.

REFERENCES

1. Li Chunyu, Chou Tsu-Wei (2003) A structural mechanics approach for the analysis of carbon nanotubes. Int J Solids Struct 40 (10): 2487-2499
2. Tserpesa, K.I. and Papanikos (2005) Finite element modelling of SWCNTs. Composites: Part B (36): 468-477
3. C. Srinivasan, "Carbon nanotubes in cancer therapy" Current Science 94, 300 (2008).
4. T. A. Hilder, J. M. Hill, "Carbon nanotubes as drug delivery nanocapsules" Current Applied Physics 8, 258 (2008).
5. Salvetat-Delmotte J, Rubio A (2002) Mechanical properties of carbon nanotubes: a fiber digest for beginners. Carbon (40): 1729-1734
6. Michele Meo, Marco Rossi (2006) Prediction of Young's Modulus of single wall carbon nanotubes by molecular-mechanics based finite element modelling, Composites Science and Technology 66: 1597-1605
7. Yakobson, B. I., Brabec, C. J. and Bernholc, J. (1996) Nanomechanics of carbon tubes: Instabilities beyond linear response. Phys Rev Lett (76): 2511- 2514
8. Lijie Chen, Qi Zhao, Hongtao Zhang, 2010. Axial buckling behavior of SWCNTs with finite element modeling. Conference of Nano/micro Engineered and molecular systems, proceedings of the 2010 5th IEEE International.
9. Buorgiorno Nardelli M, Yakobson BI, et al. (1998) Mechanism of strain release in carbon nanotubes. Phys Rev B, 57(8): R4277-4280
10. Lourie E, Cox DM, Wagner HD (1998) Buckling and collapse of embedded carbon nanotubes. Phys Rev Lett, 83: 1638-41
11. Chen L.Z. and Hui S.S Buckling and postbuckling analysis of SWCNTs in thermal environments via molecular dynamics simulation. Carbon (44): 2608-2616
12. H. Wan, F. Delale (2006) A structural mechanics approach for predicting the mechanical properties of carbon nanotubes. Meccanica (45): 43-51
13. Chunyu Li, Tsu-Wei Chou, 2004. Modeling of elastic buckling of carbon nanotubes by molecular structural mechanics approach. Mechanics of Materials.

14. E. Mohammadpour, M. Awang and M.Z Abdullah, 2011. Predicting the non-linear tensile behavior Carbon Nanotubes using Finite Element simulation. Applied Physics A (Material Science & Processing).
15. E. Mohammadpour, M. Awang and M.Z Abdullah, 2011. Predicting A Stretching Behavior of Carbon Nanotubes Using Finite Element Method. Journal of Applied Science.

APPENDICES

CONTUB v1.0 (example)

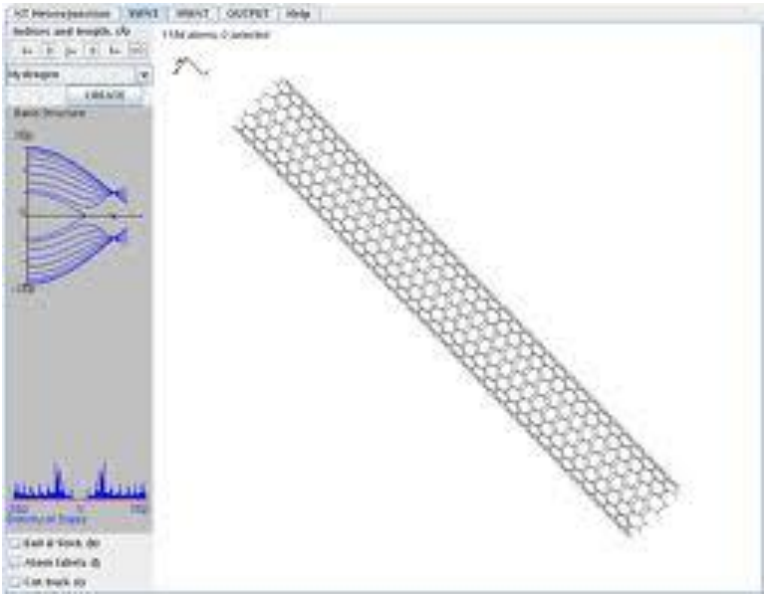

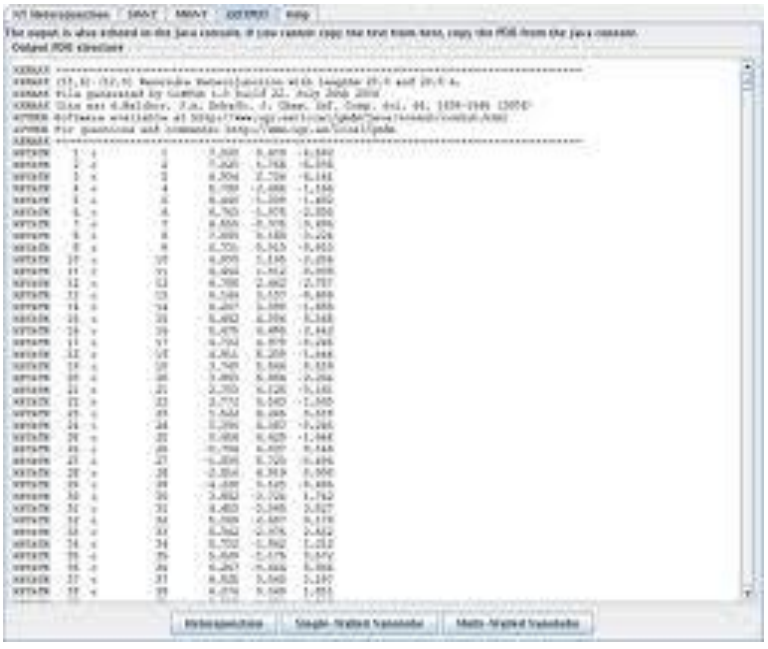

CONTUB v1.0 TO ANSYS

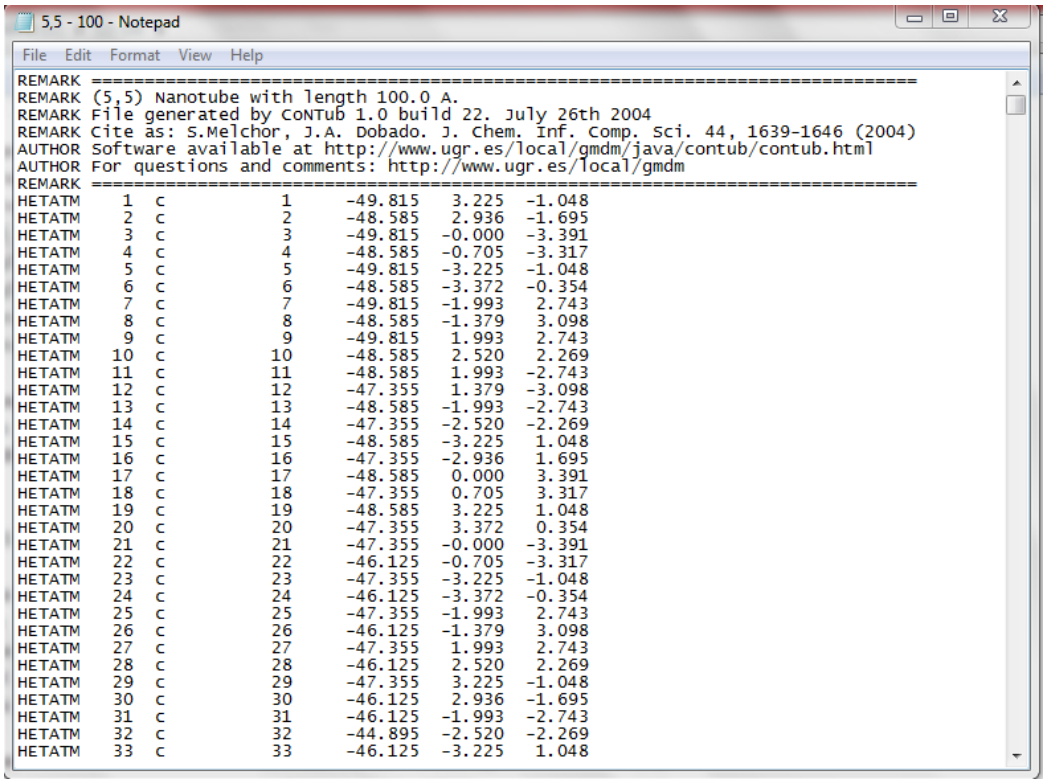

5,5 - 100 - Notepad

File Edit Format View Help

```
REMARK ========================================================================
REMARK (5,5) Nanotube with length 100.0 A.
REMARK File generated by CoNTub 1.0 build 22. July 26th 2004
REMARK Cite as: S.Melchor, J.A. Dobado. J. Chem. Inf. Comp. Sci. 44, 1639-1646 (2004)
AUTHOR Software available at http://www.ugr.es/local/gmdm/java/contub/contub.html
AUTHOR For questions and comments: http://www.ugr.es/local/gmdm
REMARK ========================================================================
HETATM    1  C           1     -49.815   3.225  -1.048
HETATM    2  C           2     -48.585   2.936  -1.695
HETATM    3  C           3     -49.815  -0.000  -3.391
HETATM    4  C           4     -48.585  -0.705  -3.317
HETATM    5  C           5     -49.815  -3.225  -1.048
HETATM    6  C           6     -48.585  -3.372  -0.354
HETATM    7  C           7     -49.815  -1.993   2.743
HETATM    8  C           8     -48.585  -1.379   3.098
HETATM    9  C           9     -49.815   1.993   2.743
HETATM   10  C          10     -48.585   2.520   2.269
HETATM   11  C          11     -48.585   1.993  -2.743
HETATM   12  C          12     -47.355   1.379  -3.098
HETATM   13  C          13     -48.585  -1.993  -2.743
HETATM   14  C          14     -47.355  -2.520  -2.269
HETATM   15  C          15     -48.585  -3.225   1.048
HETATM   16  C          16     -47.355  -2.936   1.695
HETATM   17  C          17     -48.585   0.000   3.391
HETATM   18  C          18     -47.355   0.705   3.317
HETATM   19  C          19     -48.585   3.225   1.048
HETATM   20  C          20     -47.355   3.372   0.354
HETATM   21  C          21     -47.355  -0.000  -3.391
HETATM   22  C          22     -46.125  -0.705  -3.317
HETATM   23  C          23     -47.355  -3.225  -1.048
HETATM   24  C          24     -46.125  -3.372  -0.354
HETATM   25  C          25     -47.355  -1.993   2.743
HETATM   26  C          26     -46.125  -1.379   3.098
HETATM   27  C          27     -47.355   1.993   2.743
HETATM   28  C          28     -46.125   2.520   2.269
HETATM   29  C          29     -47.355   3.225  -1.048
HETATM   30  C          30     -46.125   2.936  -1.695
HETATM   31  C          31     -46.125  -1.993  -2.743
HETATM   32  C          32     -44.895  -2.520  -2.269
HETATM   33  C          33     -46.125  -3.225   1.048
```

Nodes

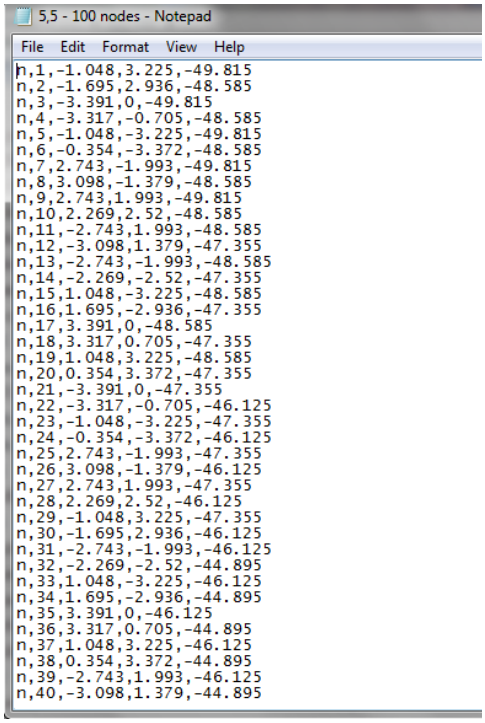

5,5 - 100 nodes - Notepad

File Edit Format View Help

```
n,1,-1.048,3.225,-49.815
n,2,-1.695,2.936,-48.585
n,3,-3.391,0,-49.815
n,4,-3.317,-0.705,-48.585
n,5,-1.048,-3.225,-49.815
n,6,-0.354,-3.372,-48.585
n,7,2.743,-1.993,-49.815
n,8,3.098,-1.379,-48.585
n,9,2.743,1.993,-49.815
n,10,2.269,2.52,-48.585
n,11,-2.743,1.993,-48.585
n,12,-3.098,1.379,-47.355
n,13,-2.743,-1.993,-48.585
n,14,-2.269,-2.52,-47.355
n,15,1.048,-3.225,-48.585
n,16,1.695,-2.936,-47.355
n,17,3.391,0,-48.585
n,18,3.317,0.705,-47.355
n,19,1.048,3.225,-48.585
n,20,0.354,3.372,-47.355
n,21,-3.391,0,-47.355
n,22,-3.317,-0.705,-46.125
n,23,-1.048,-3.225,-47.355
n,24,-0.354,-3.372,-46.125
n,25,2.743,-1.993,-47.355
n,26,3.098,-1.379,-46.125
n,27,2.743,1.993,-47.355
n,28,2.269,2.52,-46.125
n,29,-1.048,3.225,-47.355
n,30,-1.695,2.936,-46.125
n,31,-2.743,-1.993,-46.125
n,32,-2.269,-2.52,-44.895
n,33,1.048,-3.225,-46.125
n,34,1.695,-2.936,-44.895
n,35,3.391,0,-46.125
n,36,3.317,0.705,-44.895
n,37,1.048,3.225,-46.125
n,38,0.354,3.372,-44.895
n,39,-2.743,1.993,-46.125
n,40,-3.098,1.379,-44.895
```

Elements

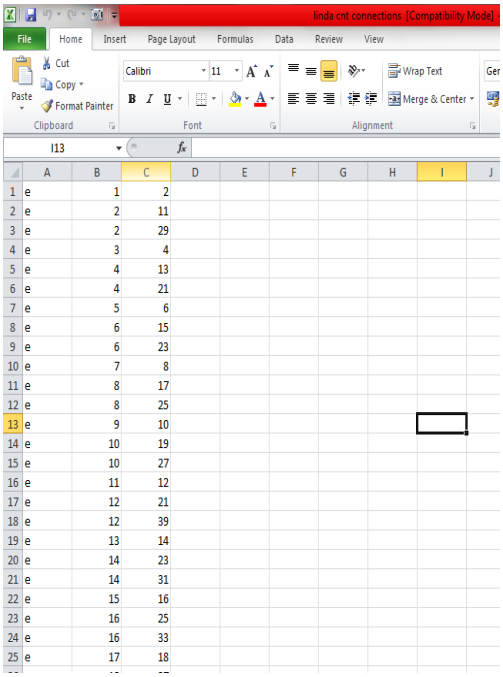

	A	B	C
1	e	1	2
2	e	2	11
3	e	2	29
4	e	3	4
5	e	4	13
6	e	4	21
7	e	5	6
8	e	6	15
9	e	6	23
10	e	7	8
11	e	8	17
12	e	8	25
13	e	9	10
14	e	10	19
15	e	10	27
16	e	11	12
17	e	12	21
18	e	12	39
19	e	13	14
20	e	14	23
21	e	14	31
22	e	15	16
23	e	16	25
24	e	16	33
25	e	17	18

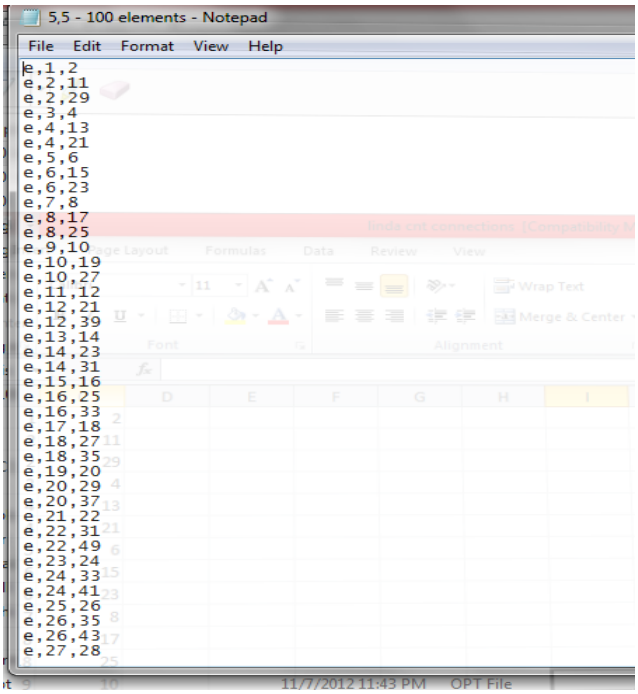

```
e,1,2
e,2,11
e,2,29
e,3,4
e,4,13
e,4,21
e,5,6
e,6,15
e,6,23
e,7,8
e,8,17
e,8,25
e,9,10
e,10,19
e,10,27
e,11,12
e,12,21
e,12,39
e,13,14
e,14,23
e,14,31
e,15,16
e,16,25
e,16,33
e,17,18
e,18,27
e,18,35
e,19,20
e,20,29
e,20,37
e,21,22
e,22,31
e,22,49
e,23,24
e,24,33
e,24,41
e,25,26
e,26,35
e,26,43
e,27,28
```

MATERIAL PROPERTIES

r_o	1.42E-10
D_e	6.03E-19
β	2.63E+10

$$E_r = D_e[1 - e^{-\beta\Delta r}] - 1$$

$$F_r = 2\beta D_e\,[1 - e^{-\beta\Delta r}]e^{-\beta\Delta r}$$

Δr	$-\beta\Delta r$	$e^{-\beta\Delta r}$	F_r
0.00E+00	0.00E+00	1	0
5.00E-11	-1.31E+00	0.26915	6.22832E-09
1.00E-10	-2.63E+00	0.07244	2.12751E-09
1.50E-10	-3.94E+00	0.0195	6.05294E-10
2.00E-10	-5.25E+00	0.00525	1.6528E-10
2.50E-10	-6.56E+00	0.00141	4.46561E-11
3.00E-10	-7.88E+00	0.00038	1.20315E-11

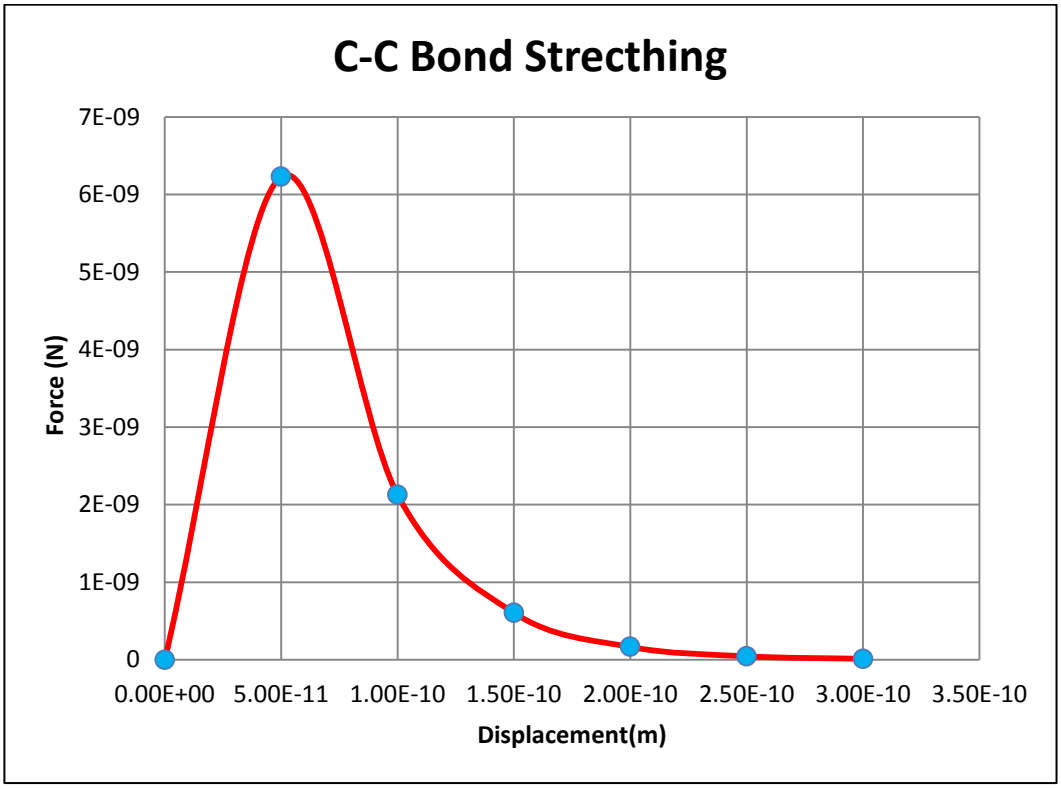

k_θ	9.00E-19
k_{sextic}	0.754
θ_0 (rad)	2.094

$$E_\theta = \frac{1}{2} k_\theta (\Delta\theta)^2 [1 + k_{sexic} \Delta\theta^4]$$

$$M(\Delta\theta) = k_\theta \Delta\theta [1 + 3k_{sextic} (\Delta\theta)^4]$$

Δθ (rad)	$(\Delta\theta)^4$	$k_\theta \Delta\theta$	M_θ
0	0	0.00E+00	0.00E+00
0.1	0.0001	9.00E-20	9.00E-11
0.2	0.0016	1.80E-19	1.81E-10
0.3	0.0081	2.70E-19	2.75E-10
0.4	0.0256	3.60E-19	3.81E-10
0.5	0.0625	4.50E-19	5.14E-10
0.6	0.1296	5.40E-19	6.98E-10
0.7	0.2401	6.30E-19	9.72E-10
0.8	0.4096	7.20E-19	1.39E-09

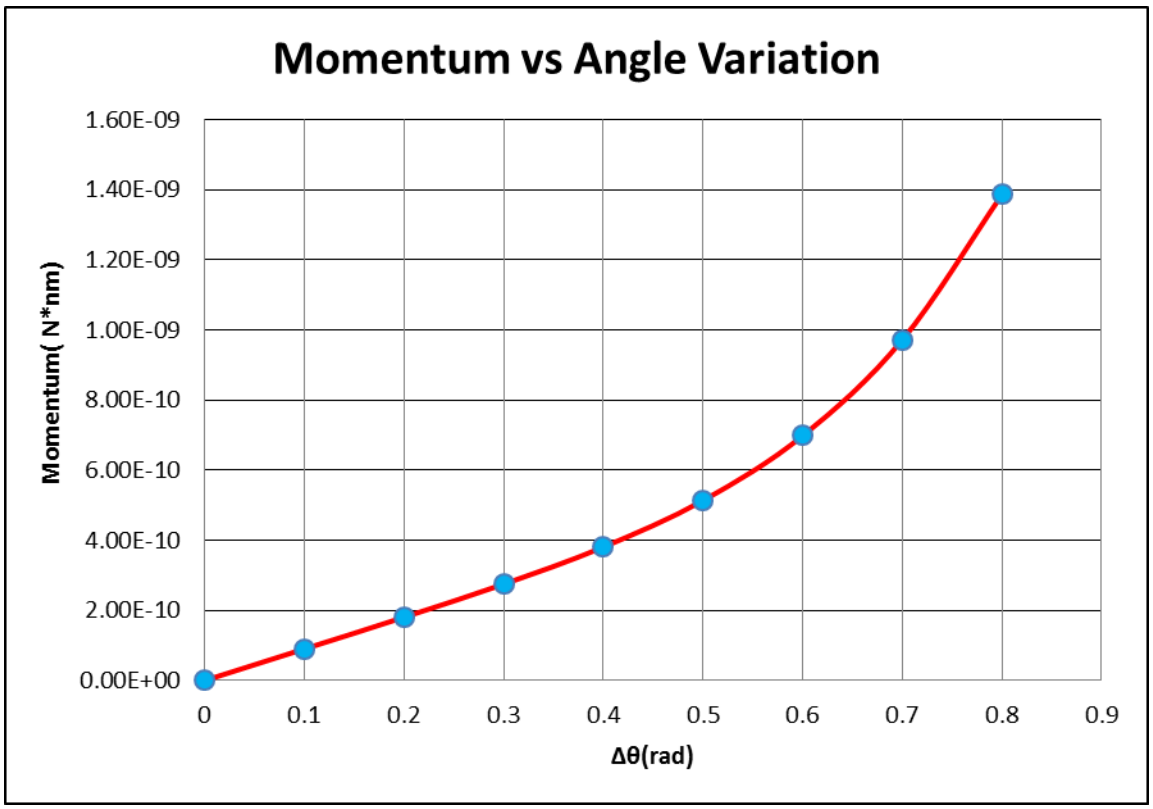

Based on calculation of molecular mechanics and continuum mechanics comparison, the diameter of the C-C bond is found to be = 0.147 nm, while the area of the whole beam (covalent bond) is = 0.115 squared nm

r0	1.42E-10

Δr	$-\beta\Delta r$	$e^{-\beta\Delta r}$	F_r	Stress $\bar{\sigma}$ F_r / A	Strain, ε Δr/ L
0.00E+00	0.00E+00	1	0	0.0000E+00	0
1.00E-12	-2.63E-02	0.9740915	8E-10	4.7283E+10	0.00704
2.00E-12	-5.25E-02	0.9488543	1.5E-09	9.0923E+10	0.01407
3.00E-12	-7.88E-02	0.924271	2.2E-09	1.3114E+11	0.02111
3.50E-12	-9.19E-02	0.9122192	2.5E-09	1.5003E+11	0.02463
4.00E-12	-1.05E-01	0.9003245	2.8E-09	1.6813E+11	0.02815
4.50E-12	-1.18E-01	0.888585	3.1E-09	1.8548E+11	0.03167
5.00E-12	-1.31E-01	0.8769985	3.4E-09	2.0210E+11	0.03519
6.00E-12	-1.58E-01	0.8542768	3.9E-09	2.3323E+11	0.04222
7.00E-12	-1.84E-01	0.8321438	4.4E-09	2.6170E+11	0.04926
8.00E-12	-2.10E-01	0.8105842	4.9E-09	2.8766E+11	0.0563
9.00E-12	-2.36E-01	0.7895833	5.3E-09	3.1127E+11	0.06334
1.00E-11	-2.63E-01	0.7691264	5.6E-09	3.3269E+11	0.07037
1.10E-11	-2.89E-01	0.7491995	5.9E-09	3.5204E+11	0.07741
1.20E-11	-3.15E-01	0.7297889	6.2E-09	3.6946E+11	0.08445
1.30E-11	-3.41E-01	0.7108812	6.5E-09	3.8507E+11	0.09148
1.40E-11	-3.68E-01	0.6924633	6.7E-09	3.9899E+11	0.09852
1.50E-11	-3.94E-01	0.6745227	7E-09	4.1132E+11	0.10556
2.00E-11	-5.25E-01	0.5915554	7.7E-09	4.5268E+11	0.14075
3.00E-11	-7.88E-01	0.4549808	7.9E-09	4.6459E+11	0.21112
4.00E-11	-1.05E+00	0.3499377	7.2E-09	4.2620E+11	0.28149
5.00E-11	-1.31E+00	0.2691463	6.2E-09	3.6854E+11	0.35186
1.00E-10	-2.63E+00	0.0724398	2.1E-09	1.2589E+11	0.70373
1.50E-10	-3.94E+00	0.0194969	6.1E-10	3.5816E+10	1.05559
2.00E-10	-5.25E+00	0.0052475	1.7E-10	9.7799E+09	1.40746
2.50E-10	-6.56E+00	0.0014124	4.5E-11	2.6424E+09	1.75932
3.00E-10	-7.88E+00	0.0003801	1.2E-11	7.1192E+08	2.11119

MISO			
TBPT	DEFI	0	0
TBPT	DEFI	0.0007	4.7E+10
TBPT	DEFI	0.00141	9.1E+10
TBPT	DEFI	0.00211	1.3E+11
TBPT	DEFI	0.00246	1.5E+11
TBPT	DEFI	0.00281	1.7E+11
TBPT	DEFI	0.00317	1.9E+11
TBPT	DEFI	0.00352	2E+11
TBPT	DEFI	0.00422	2.3E+11
TBPT	DEFI	0.00493	2.6E+11
TBPT	DEFI	0.00563	2.9E+11
TBPT	DEFI	0.00633	3.1E+11
TBPT	DEFI	0.00704	3.3E+11
TBPT	DEFI	0.00774	3.5E+11
TBPT	DEFI	0.00844	3.7E+11
TBPT	DEFI	0.00915	3.9E+11